

รูปแบบการไหลของการไหลแบบหลายภูมิภาคของของเหลว
ในไมโครรีแอกเตอร์ที่มีโครงสร้างนำทางต่างกันและการปรับเปลี่ยนพื้นผิว

นางสาวชญาตุ่ม โฉมิตานนท์

วิทยานิพนธ์นี้เป็นส่วนหนึ่งของการศึกษาตามหลักสูตรปริญญาวิทยาศาสตรดุษฎีบัณฑิต

สาขาวิชาวิศวกรรมเคมี ภาควิชาวิศวกรรมเคมี

คณะวิศวกรรมศาสตร์ จุฬาลงกรณ์มหาวิทยาลัย

ปีการศึกษา 2555

ลิขสิทธิ์ของจุฬาลงกรณ์มหาวิทยาลัย

บทคัดย่อและแฟ้มข้อมูลฉบับเต็มของวิทยานิพนธ์ตั้งแต่ปีการศึกษา 2554 ที่ให้บริการในคลังปัญญาจุฬาฯ (CUIR)

เป็นแฟ้มข้อมูลของนิสิตเจ้าของวิทยานิพนธ์ที่ส่งผ่านทางบัณฑิตวิทยาลัย

The abstract and full text of theses from the academic year 2011 in Chulalongkorn University Intellectual Repository(CUIR) are the thesis authors' files submitted through the Graduate School.

FLOW PATTERN OF LIQUID MULTIPHASE FLOW IN MICROREACTOR
WITH DIFFERENT GUIDELINE STRUCTURES
AND SURFACE MODIFICATION

Miss Chayanoot Kositanont

A Dissertation Submitted in Partial Fulfillment of the Requirements
for the Degree of Doctor of Engineering Program in Chemical Engineering

Department of Chemical Engineering

Faculty of Engineering

Chulalongkorn University

Academic Year 2012

Copyright of Chulalongkorn University

ชญาตม์ โหมิตานนท์ : รูปแบบการไหลของการไหลแบบหลายวัฏภาคของของเหลวในไมโครรีแอกเตอร์ที่มีโครงสร้างนำทางต่างกันและการปรับเปลี่ยนพื้นผิว. (FLOW PATTERN OF LIQUID MULTIPHASE FLOW IN MICROREACTOR WITH DIFFERENT GUIDELINE STRUCTURES AND SURFACE MODIFICATION) อ.ที่ปรึกษาวิทยานิพนธ์หลัก : ศ.ดร. สุทธิชัย อัสสะบารุงรัตน์, อ.ที่ปรึกษาวิทยานิพนธ์ร่วม : Professor Tomohiko Tagawa, ผศ.ดร. สมพงษ์ พุทธิวิสุทธิศักดิ์, 98 หน้า.

การไหลแบบขนานทำให้สามารถแยกผลิตภัณฑ์ที่ทางออกของไมโครรีแอกเตอร์ได้โดยง่าย และดังนั้นจึงสามารถลดความต้องการบำบัดขั้นหลังได้ด้วย งานวิจัยนี้จึงได้นำโครงสร้างนำทางและการปรับเปลี่ยนพื้นผิวโดยใช้ปฏิกิริยา silanization มาใช้เพื่อรักษารูปแบบการไหลสองเฟสของสารอินทรีย์และน้ำในไมโครรีแอกเตอร์แก้วให้เป็นแบบขนานและทำให้เสถียร ผลของโครงสร้างนำทางและการปรับเปลี่ยนพื้นผิวที่มีต่อรูปแบบการไหลได้ทำการศึกษาโดยใช้พลศาสตร์ของไหลเชิงคำนวณ (computational fluid dynamics, CFD) ซึ่งพบว่าสามารถทำนายรูปแบบการไหลได้ดีเมื่อเทียบกับผลจากการทดลอง สำหรับไมโครรีแอกเตอร์แบบท่อตรงนั้น พบว่าเส้นแบ่งสถานะเสถียรมากขึ้นและเปลี่ยนเป็นรูปโค้งเมื่อใช้โครงสร้างนำทาง ซึ่งจะพบว่า CFD สามารถวิเคราะห์บทบาทของโครงสร้างที่มีต่อพัฒนาการของการไหลได้ เมื่อปรับปรุงไมโครรีแอกเตอร์ที่มีโครงสร้างนำทางโดยใช้การปรับเปลี่ยนพื้นผิว พบว่าของไหลใช้เวลาน้อยลงเพื่อเข้าสู่รูปแบบการไหลที่เสถียรและไหลอยู่ในทางตั้งแต่เริ่มป้อนสาร เมื่อเปลี่ยนอัตราการไหลและสัดส่วนของของไหล พบว่าเกิดความไม่เสถียรที่อัตราการไหลสูงและต่ำ ซึ่งที่อัตราการไหลสูงนั้นสามารถทำให้เส้นแบ่งสถานะเสถียรได้โดยปรับสัดส่วนของอัตราการไหล การปรับเปลี่ยนพื้นผิวยังสามารถเปลี่ยนแปลงรูปแบบการไหลจากแบบขนานเป็นแบบ slug ที่อัตราการไหลต่ำได้ ทั้งยังพบว่าความกว้างและความโค้งของไมโครรีแอกเตอร์มีผลต่อรูปแบบการไหลด้วย ในไมโครรีแอกเตอร์แบบท่อโค้งโครงสร้างนำทางไม่สามารถทำให้เส้นแบ่งสถานะเสถียรได้ในสภาวะการไหลที่ทำกรคำนวณในทางตรงกันข้ามการปรับเปลี่ยนพื้นผิวสามารถดึงเส้นแบ่งสถานะไว้ที่ตรงกลางช่องทางการไหลและรักษารูปแบบการไหลแบบขนานไว้ได้ด้วยความเร็วสูง

ภาควิชา.....วิศวกรรมเคมี.....ลายมือชื่อ.....
 สาขาวิชา.....วิศวกรรมเคมี.....ลายมือชื่อ อ.ที่ปรึกษาวิทยานิพนธ์หลัก.....
 ปีการศึกษา.....2555.....ลายมือชื่อ อ.ที่ปรึกษาวิทยานิพนธ์ร่วม.....
 ลายมือชื่อ อ.ที่ปรึกษาวิทยานิพนธ์ร่วม.....

5171841621 : MAJOR CHEMICAL ENGINEERING

KEYWORDS : MICROSTRUCTURE / MULTIPHASE FLOW / GUIDELINE
STRUCTURE / SURFACE MODIFICATION / CFD

CHAYANOOT KOSITANONT : FLOW PATTERN OF LIQUID
MULTIPHASE FLOW IN MICROREACTOR WITH DIFFERENT
GUIDELINE STRUCTURES AND SURFACE MODIFICATION. ADVISOR :
PROF. SUTTICHAJ ASSABUMRUNGRAT, Ph.D., CO-ADVISOR : PROF.
TOMOHIKO TAGAWA, Ph.D., ASST. PROF. SOMPONG PUTIVISUTISAK,
Ph.D., 98 pp.

A parallel multiphase flow in microchannel offers simple phase separation at the exit and hence, reduces the post-treatment requirements. Guideline structure and surface modification by silanization was therefore, introduced to stabilize and maintain organic-aqueous two phase parallel flow in a glass microchannel. The effects of guideline structure and surface modification on water-toluene flow pattern were investigated using computational fluid dynamics (CFD). The CFD simulation can well predict the flow patterns observed from the experiment. In straight microchannel, with the presence of guideline structure, the interface became more stable with curve shape. The role of guideline structure on the flow development was analyzed. With surface modification, the stable interface was pinned near the center of the microchannel with guideline structure. The fluids required less time to reach the stable flow pattern and could be maintained in their corresponding paths since feeding. Flow rate and flow ratio were varied to investigate the flow behaviors. The instabilities were observed at higher and lower flow rates. At higher flow rate, the interface stability could be obtained by adjusting the flow rate ratio. The parallel-slug flow pattern transition, which occurs at low flow rate, could be altered by surface modification. The effects of channel width and curve radius were demonstrated. In curved microchannel, the guideline could not stabilize the interface at the simulation flow conditions. In contrast, the surface modification could fix the interface at the channel center and maintain the parallel flow pattern at high flow rate.

Department : Chemical Engineering Student's Signature

Field of Study : Chemical Engineering Advisor's Signature

Academic Year : 2012 Co-advisor's Signature

Co-advisor's Signature

ACKNOWLEDGEMENTS

The author would like to express highly appreciation to her thesis advisor, Professor Suttichai Assabumrungrat, for his wisdom and guidance in research study and life attitude. She also wishes to thank her co-advisor, Professor Tomohiko Tagawa, for good advice and kind assistance, especially during her stay in Japan and, Assistant Professor Sompong Putivisutisak, for his valuable suggestion and support. Moreover, she would like to thank to Associate Professor Muenduen Phisalaphong as the chairman, Associate Professor Bunjerd Jongsomjit, Assistant Professor Anongnat Somwangthanaroj and Dr. Thana Sornchamni as the members of the thesis committee.

She also would like to acknowledge for the financial support from Dusadeepipat scholarship from Chulalongkorn University and the great opportunity from Nagoya University Program for Academic Exchange (NUPACE).

She would like to give special thanks to Assistant Professor Hiroshi Yamada for useful help and Associate Professor Susumu Nii, Hajime Ito and members in Nagoya University who gave her supports while she was staying in Japan.

Finally, the author would like to express great gratitude to her parents and brother. She cannot completely achieve a success without the support and encouragement from her family.

CONTENTS

	Page
ABSTRACT (THAI).....	iv
ABSTRACT (ENGLISH).....	v
ACKNOWLEDGEMENTS.....	vi
CONTENTS.....	vii
LIST OF TABLES.....	ix
LIST OF FIGURES.....	x
NOMENCLATURES.....	xiii
CHAPTER	
I INTRODUCTION.....	1
1.1 Background.....	1
2.2 Research objectives.....	3
2.3 Research scopes.....	3
II THEORY.....	5
2.1 Microreactor.....	5
2.2 Multiphase flow.....	8
2.3 CFD.....	13
III LITERATURE REVIEWS.....	19
3.1 Two-phase flow pattern.....	19
3.2 Parallel flow stabilization in microreactor.....	25
3.3 CFD application in multiphase microreactor.....	29
3.4 Multiphase flow in small curved channel.....	31
IV NUMERICAL MODELLING.....	33
4.1 Commercial software validation.....	33
4.1.1 2D parallel flow pattern.....	34
4.1.2 2D slug size.....	35
4.1.3 3D flow pattern and slug size.....	36
4.2 Microreactor simulation.....	39
4.2.1 2D straight microchannel.....	39
4.2.2 3D curved microchannel.....	44

CHAPTER	Page
V RESULTS AND DISCUSSION.....	50
5.1 Effect of guideline structure in straight microchannel.....	50
5.2 Effect of surface modification in straight microchannel.....	58
5.3 Effect of guideline structure and surface modification in curved microchannel.....	66
VI CONCLUSIONS AND RECOMMENDATIONS.....	81
6.1 Conclusions.....	81
6.1.1 Guideline structure.....	81
6.1.2 Surface modification.....	81
6.1.3 CFD method.....	82
6.2 Recommendations.....	82
REFERENCES.....	84
APPENDICES.....	93
APPENDIX A SIMULATION MATERIAL PROPERTIES.....	94
APPENDIX B SLUG SIZE CALCULATION.....	95
APPENDIX C LIST OF PUBLICATIONS.....	97
C.1 International publications.....	97
C.2 International conferences.....	97
VITA.....	98

LIST OF TABLES

TABLE		Page
3.2	Gas-liquid flow pattern in microchannels (Weinmueller et al., 2009)	21
4.1	3D validation water slug length	38
4.2	Guideline structure length	40
5.1	Flow patterns after bend in microchannel without modification	68
5.2	Volume fractions at position a-e of parallel, annular and phase switch flow patterns in curved microchannel without modification ..	70
5.3	Flow patterns after bend in microchannel with guideline structure ..	71
5.4	Volume fractions at position a-e of parallel, annular and phase switch flow patterns in curved microchannel with guideline structure	74
5.5	Volume fractions at position a-e cross section of parallel flow patterns in curved microchannel with surface modification	76
5.6	Velocity vectors at position a, c and e cross section in curved microchannel without modification	78
A	Simulation material properties	94
B	Simulation and reported slug length in Figure 4.4	96

LIST OF FIGURES

FIGURE		Page
2.1	Hierarchical assembly of microreactors (Ehrfeld et al., 2000).....	6
2.2	A sessile drop with contact angle and surface tensions.....	11
3.1	Flow patterns of liquid-liquid two-phase vertical upward flow in pipes (Lin and Tavlarides, 2009).....	20
3.2	Observed oil-water flow patterns in a horizontal 0.0254 m pipe (Al-Yaari et al., 2010).....	20
3.3	Micro-PIV images from: (a) bubbly, (b) regularly ordered bubbly flow, (c) wedging, (d) slug, and (e) annular flow (Weinmueller et al., 2009).....	22
3.4	Photographs of oil-water flow patterns in microchannel initially saturated with oil: (a) droplet flow, (b) slug flow, and (c) annular flow (the arrow indicates the flow direction) (Salim et al., 2008).....	23
3.5	Snapshot of parallel flows that have smooth interface in microchannel (Zhao et al., 2006).....	23
3.6	Liquid-liquid flow patterns in microfabricated systems diagram with transition lines and operating conditions for different literature data (Günther and Jensen, 2006).....	24
4.1	2D validation three inlet microchannel.....	34
4.2	2D simulated stable stratified flow of the air (dark gray) and water (light gray) at superficial velocities of 20 and 0.4 m/s, respectively..	35
4.3	2D simulated slug flow of air (dark gray) and water (light gray) at superficial velocities of 0.0694 and 0.0764 m/s, respectively.....	35
4.4	Comparison of the 2D slug length between the simulated results and the results reported by Guo and Chen (2009).....	36
4.5	3D validation model with grids.....	37
4.6	Simulated slug flows of water (dark gray) and kerosene (light gray) at flow rates of 10 and 20 ml/h, respectively.....	37

FIGURE	Page
4.7 Simulated parallel flows at each phase flow rates of 150 ml/h.....	38
4.8 Microchannel with guideline structure (model A).....	39
4.9 Microchannel model A with grids.....	40
4.10 Water and organic parts in the modified surface microchannel.....	41
4.11 Pressure-based segregated algorithm (ANSYS Inc., 2009).....	42
4.12 Contact angles of water (clear phase) in toluene (dyed phase) on the glass surface before (left) and after (right) silanization.....	43
4.13 Curved microchannel with 0.5 mm curvature radius (a) top view and (b) cross section view.....	45
4.14 Meshed microchannel with guideline structure (a) outline, (b) inlet, (c) wall, (d) curve and (e) wall with interior meshes.....	46
4.15 Cross section plane position.....	49
5.1 (a) Simulated stable parallel flow pattern of model A at 0.0148 s and (b) experimental observation.....	51
5.2 Flow development in model A.....	52
5.3 Flow development in model B.....	52
5.4 Flow development in model C.....	53
5.5 Simulated flow pattern of model A at (a) 0.0025 ml/min, (b) 0.0005 ml/min.....	54
5.8 Movement of the forefront part of toluene in model A passing each guideline structure in parallel flow pattern.....	54
5.7 Movement of the forefront part of toluene in model A passing each guideline structure at near inlet in slug flow pattern which broken at (a) the front edge and (b) the back edge.....	55
5.8 Velocity vectors at 0.01 ml/min in model A, B and C.....	57
5.9 Velocity vectors at 0.0005 ml/min of a moving slug in model A.....	58
5.10 Flow development in the unmodified microchannel at the same phase feed flow rate at 0.01 ml/min.....	59

FIGURE	Page
5.11	Flow development in the modified microchannel at the same phase feed flow rate at 0.01 ml/min..... 60
5.12	Simulated flow patterns at the same phase feed flow rate at 0.01 ml/min of (a) unmodified microchannel, (b) modified surface microchannel..... 61
5.13	Simulated flow pattern of modified microchannel at 0.0005 ml/min. 61
5.14	Simulated flow patterns of unmodified microchannel at different phase feed flow rates..... 62
5.15	Simulated flow patterns of modified microchannel at different phase feed flow rates..... 63
5.16	Simulated flow patterns of modified microchannel at different feed flow rate ratio with fixed organic phase flow rate of 0.02 ml/min..... 64
5.17	Simulated flow patterns of modified microchannel at different feed flow rate ratio with fixed organic phase flow rate of 0.03 ml/min..... 64
5.18	Simulated flow patterns of unmodified microchannel at the phase flow rate of 0.02 ml/min with (a) a half width, (b) a normal width and (c) a double width..... 65
5.19	Simulated flow patterns of modified microchannel at the phase flow rate of 0.02 ml/min with (a) a half width, (b) a normal width and (c) a double width..... 66
5.20	Volume fractions in curved microchannel without modification at position b of (a) 0.025 and (b) 1 ml/min with outer water lane..... 67
5.21	Flow patterns in plain cured microchannel of phase feed flow rates at (a) 0.025 ml/min with outer toluene, (b) 0.025 ml/min with outer water, (c) 0.5 ml/min with outer toluene, (d) 0.5 ml/min with outer water and (e) 1 ml/min with outer water..... 68

FIGURE	Page	
5.22	Flow patterns in cured microchannel with guideline structure of phase feed flow rates at (a) 0.025 ml/min with outer toluene, (b) 0.025 ml/min with outer water, (c) 0.5 ml/min min with outer toluene, (d) 0.5 ml/min min with outer water and (e) 1 ml/min with outer water.....	72
5.23	Flow patterns in curved microchannel with surface modification of phase feed flow rates at (a) 0.025 ml/min with outer toluene and (b) 1 ml/min with outer water.....	75
5.24	Flow pattern at 3 ml/min in microchannel with surface modification in (a) top view and (b) cross section at position e.....	79
5.25	Flow pattern at 1 ml/min in plain microchannel with 3 mm curvature radius in (a) top view and (b) cross section at position e....	80
B	Water volume fraction at water and kerosene flow rates of 10 and 20 ml/h, respectively.....	96

NOMENCLATURE

Bo	Bond number
Ca	Capillary number
d	Channel depth
d_H	Hydraulic or equivalent diameter
De	Dean number
f	Friction factor
F	Surface tension force
g	Gravitational acceleration
L	Channel length
m	Mass
n	Surface normal
\hat{n}	Unit surface normal
\hat{t}	Unit vector tangential
P	Phase pressure
p	Pressure
R	Curve radius
Re	Reynolds number
S	Additional source

t	Time
u	Linear or superficial velocity
v	Mean velocity
We	Weber number

Greek letters

α	Volume fraction
κ	Curvature
μ	Viscosity
θ	Contact angle
ρ	Density
σ	Surface tension

Subscripts

A	Air
L	Liquid phase
O	Organic phase
S	Solid phase
V	Vapor phase
w	Wall
W	Water

CHAPTER I

INTRODUCTION

1.1 Background

Microreaction technology (MRT), an important approach for process intensification, offers some outstanding advantages in comparison to conventional reactor systems such as intensifying mass and heat transport, improving flow patterns, increased process safety and improved selectivity. Recently, microreaction technology has attracted attention from many researchers and become of commercial use in some industries such as vehicles, refrigeration systems, fuel cells, electronics, aerospace, pharmaceutical, semiconductor and petrochemical (Hessel et al., 2005, Kockmann, 2006). Microreactors are realized as miniaturized reaction systems with typical channel or chamber widths in the range of 10-500 μm (Lowe and Ehrfeld., 1999). Many gas or liquid phase reactions have been performed in microreactors. With decreasing dimensions, the surface-to-volume ratio increases, and therefore the specific surfaces and the specific interfaces of multiphase systems are increased (Ehrfeld et al., 2000).

In the chemical industry, there are numerous reactions that are carried out on a large scale with strongly exothermic and involve two-phase liquid-liquid systems in consequence of the immiscibility of the participating fluids (Dummann et al., 2003). For these liquid-liquid systems such as the organic-aqueous reaction systems, microreactor which possesses a large surface-to-volume ratio can reduce the mass transfer limitations involved.

Due to the large surface-to-volume ratio, surface effects become important. Therefore multiphase flow with many interfaces in microstructures shows different flow patterns deviated from those observed in macro-scale systems. For liquid-liquid two-phase flow in microchannel, the common flow patterns are slug flow and parallel

or laminar flow. It is practical to obtain a stable multiphase laminar flow in microchannel which can provide a phase separation of the product mixture at the exit and then reduces the post-treatment unit operation requirements. This microunit with the phase separation was expected to use in a design of continuous microsystem. A microreactor with guideline structure has been proposed in order to stabilize the laminar flow for multiliquid phase systems (Surmeian et al., 2002, Tokeshi et al., 2002, Maruyama et al., 2004, Tagawa et al., 2007). Besides the use of guideline structure, surface modification is another proposed method (Hibara et al., 2002, Maruyama et al., 2003, Smirnova et al., 2006). Hydrophilic nature of glass surface of organic phase part could be changed to be hydrophobic by silanization.

Besides the straight channel, the curved channel is very common because of their high heat and mass transfer, compactness and narrow residence time distributions (Kumar et al., 2007). Therefore, the flow characteristic in curved microchannel and the effect of the flow parallelize techniques are also interesting.

Computational fluid dynamics (CFD) is a powerful technique applying numerical methods for analyzing the flow and performance of process equipment. It has been recently applied to engineering design of components and systems in many application fields. There are many advantages of CFD over experimental approaches. It can reduce cost as well as time in engineering process. Moreover, the microfluidic behavior can be studied comprehensively. There are many commercial CFD software codes available and among them, FLUENT is one of the widely-used commercial CFD codes based on finite volume method. In order to model the immiscible fluid flow, there are many available approaches. Volume of fluid method (VOF) is a common surface tracking technique existing in FLUENT. Thus, it is interesting to apply the CFD method to study the flow characteristics of multiphase liquid system in both straight and curved microreactors with guideline structures and surface modification. Therefore, an optimum design with desired separation function can be determined with less effort on experimental approach that high cost microreactor systems are fabricated.

1.2 Research objectives

The research objectives are

1. To determine the effect of geometry of guideline structure on the flow pattern and phase separation.
2. To determine the effect of surface modification on the flow pattern and phase separation in microchannel with guideline structure.
3. To evaluate the effect of operating condition and channel size on the flow pattern and phase separation in microreactor with guideline structure.
4. To examine the effect of bend on the flow pattern in microchannel.
5. To investigate the flow pattern, flow development and velocity fields in microreactor by using a commercial CFD software.

1.3 Research scopes

The scopes of this research are as follows.

1. The models of microreactors without guideline structure and with guideline structures that are different in length and interval are simulated to analyze the effect of guideline structure on multiphase liquid flow pattern at various flow conditions.
2. The surface modification effect on multiphase liquid flow pattern at various flow conditions is studied by altering the contact angle, which is observed from the experiment, specified in the simulation setting procedure.
3. The microchannel with 180° bend is used in simulation to investigate the effect of curvature and outer-inner phase arrangement in plain, guideline wall equipped and modified surface cases at various flow conditions.
4. The simulation are carried out in 2D and 3D space for symmetry and asymmetry geometries, respectively, using commercial software FLUENT with VOF model for surface tracking.
5. The simulation accuracy is validated both in 2D and 3D by comparing the simulation results to the published experimental and simulation results.

6. The microchannel and guideline structure dimensions of simulation models are based on laboratory previous work and commercial microchannels.
7. The stable interface in this research results is considered as the smooth interface that is not changed with time.

CHAPTER II

THEORY

2.1 Microreactor

In the chemical industry, process intensification is a current trend to significantly increase the process efficiency by reducing energy consumption and/or byproduct formation as well as decreasing equipment size. Microreaction technology is recognized as one essential approach for process intensification in the chemical and process industry.

Microreactors are defined as miniaturized reaction systems fabricated by using methods of microtechnology and precision engineering (Ehrfeld et al., 2000). Hierarchical assembly of microreactors, as evidenced for micromixer components, is shown in Figure 2.1. In a continuous flow system, the smallest parts are microstructures (microchannels in the most cases) which are combined to an array. The array is connected with headers or inlet and outlet parts. A single or multiple flow channel configuration of different geometric nature is termed element. An element with base material for supporting and connected fluid lines is unit. The units may be formed to a stack to increase throughput. A unit embedded either in a housing or between two end caps is referred to device. A system can be performed by combining several units within one housing or by connecting devices which is referred to as components in this case. Any parallel or serial interconnection of components, systems or mixed combinations may be termed set-up or plant, depending on whether applied in laboratory or industry.

The components and systems can be used as various unit operations such as micromixers, micro heat exchangers, microseparators and microreactors. The multifunctional reactors can be also considered as one technique of process intensification. Thus the integration of these more than one unit operations as the

multifunctional reactor concept results in fewer and more compact units with increased process efficiency.

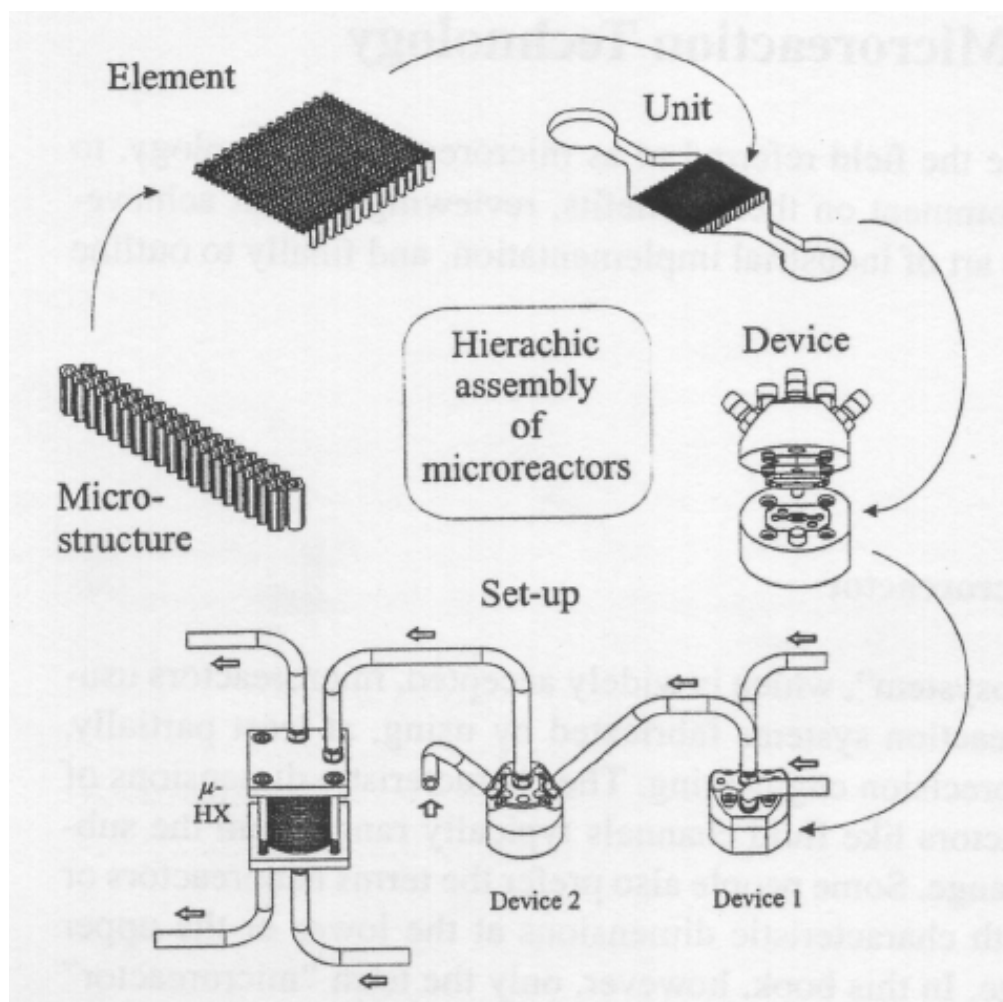


Figure 2.1 Hierarchical assembly of microreactors (Ehrfeld et al., 2000)

For fabrication of microreactors, several materials such as quartz, glass, silicon, metals and polymers have been used to construct the reactor. A range of microfabrication methods are available, for example, wet chemical etching, dry etching, LIGA (a German acronym for Lithographie, Galvanoformung, Abformung (Lithography, Electroplating, and Molding)) process, injection molding, advanced mechanical techniques and laser micromachining. The technique has to be chosen by

considering factors such as material choice, process cost, process time, accuracy, reliability and access.

There are many advantages of microreactors. For analysis application, the miniaturized devices need less materials, space and energy, produce less waste, often have shorter response times and allow the integration for increasing the system performance. For chemical production, reducing the dimension in microreactors causes the small diffusion path and the large surface to volume ratio which enhance the mass and heat transfer performance compared to conventional reactors. In fast multiphase reaction cases, the rate and selectivity can be greatly influenced by the transport of reagents within and across phases. The microfluidic device also offers a large interface area to volume ratio and increases the mass transfer at the interface. According to the decreasing of volume, the large-sized batch process can be replaced by continuous flow microsystems and the material hold-up is decreased which increases process safety. In production scale systems of multiple microreactors, the failed reactor can be isolated and replaced while the production is continued with other parallel units and the small quantity of chemicals is released. These should allow distributed point-of-use synthesis of chemicals with storage and shipping limitations. The shorter residence time decreases the byproduct formation which leads to higher selectivity. The experimentation and introduction of new chemicals can be performed with safety and low costs. An increased production capacity is completed by numbering-up with no need to scale-up. This approach can maintain basic unit designed characteristics which can eliminate costly redesign and pilot plant experiments, thus reducing the development time from laboratory to commercial production. Assembly of microreactors also results in higher production flexibility for varying production demand. Moreover a variety of reactions can be achieved by modifying a piping network.

The two restrictions for microreaction technology are the possibility to fabricate the small structures with reasonable costs and the probability of fouling and blocking. The first problem has been broadened by improving fabrication potentials.

But the fouling and blocking problem still remain and should be considered (Kockmann, 2006).

2.2 Multiphase flow

Multiphase flows form when two or more partially or immiscible fluids are brought in contact and subjected to a pressure gradient. In ordinarily sized large tubes as well as in a few mm order tubes, the two-phase flow patterns are dominated in general by gravity with less surface tension effects. On the other hand, in microsystems, the surface-to-volume ratio increases and surface effects become important. Factors such as surface tension or wall wetting are more dominant compared to volume forces like gravity, pressure, or momentum. Thus multiphase flow in microstructures with many interfaces shows different behavior and characteristic from in macro-scale systems. This detailed knowledge of the hydrodynamics in the microchannels is required to design a microreactor and to define the conditions for a specific system.

In microchannels, the interfacial tension, the inertia and the viscosity are the most important forces controlling the interface. The interfacial tension and the viscous forces control the flow patterns because of the channel diameter dependence (Akbar et al., 2003, Kreutzer et al., 2005) and the gravity and inertia effects are normally negligible (Atencia and Beebe, 2005). The proportion of the forces can be quantified by dimensionless numbers.

The dimensionless Reynolds (Re) number (Eq. 2.1) expresses the ratio of inertia forces which are resistant to change or motion to viscous forces, which arising from viscous effects in fluid flow, that tend to produce random eddies, vortices and other flow instabilities. This parameter is naturally small in micro-scale case due to inertial effects are small compared to viscous effects.

$$Re = \frac{\rho \cdot u \cdot d_H}{\mu} \quad (2.1)$$

where, ρ is the fluid density, u is the linear or superficial velocity, d_H is the hydraulic or equivalent diameter of the channel, and μ is the dynamic fluid viscosity.

Weber (We) number (Eq. 2.2) expresses the ratio of inertia forces to interfacial tension. The interfacial tension tends to minimize the interfacial area, while inertia force extend and drag the interface downstream. Although the diameter length is small, Weber number can be large due to the strong dependence on the velocity. Rezkallah and Zhao (1995), Rezkallah (1996) and Lowe and Rezkallah (1999) developed two-phase gas-liquid flow transition mapping based on phase Weber numbers.

$$We = \frac{u^2 \cdot d_H \cdot \rho}{\sigma} \quad (2.2)$$

where σ is interfacial tension or liquid-liquid surface tension.

Capillary (Ca) number (Eq. 2.3) expresses the ratio of viscous shear forces to elongate an interface to the interfacial tension forces which act to minimize interfacial area between the phases. This number was used to explain many works in microscale because the viscous forces and the interfacial tension are the dominating forces in this small scale. A stable elongated interface between the two phases occurs when the viscous forces are equal to or greater than the interfacial forces. The Capillary number can also be determined by dividing the Weber number by the Reynolds number. Raddy et al. (2005) minimized the interfacial tension in DNA extraction to obtain a stable stratified flow in the microchannels by adding surfactant and explained in the term of Capillary number. Liu and Wang (2009) investigated gas-liquid Taylor flow in vertical noncircular capillaries using CFD. Bubble size and shape, liquid film thickness, velocity field and two-phase relative velocity, were studied as functions of capillary number.

$$Ca = \frac{\mu \cdot u}{\sigma} \quad (2.3)$$

The importance of gravity with respect to interfacial forces is described by the Bond (Bo) number (Eq. 2.4).

$$Bo = \frac{(\Delta\rho) \cdot g \cdot d_H^2}{\sigma} \quad (2.4)$$

where, $\Delta\rho$ is the density difference between the liquid and the gas and g is the gravitational acceleration. The interfacial forces often dominate over the influence of gravity in the microscale, the Bond number is much less than 1 (Günther and Jensen, 2006).

Dean (De) number (Eq. 2.5) expresses the ratio of the square root of the product of the inertial and centrifugal forces to the viscous force. It is used to explain the fluid flow in the curved channel which the centrifugal force induce the instability. The secondary flows or Dean vortices are results of this centrifugal force. It can measure the secondary flow magnitude.

$$De = Re \sqrt{\frac{d_H}{2R}} \quad (2.5)$$

where, R is the curvature radius.

To characterize the surface wettability which is important property in the Microsystems, the contact angle is used. It is defined as the angle between the wall and the tangent to the interface of the fluids. In a given system of solid, fluids at a given temperature and pressure, there is a unique equilibrium contact angle. In practical, contact angle hysteresis, which is a range of advancing contact angle to receding contact angle, is observed. The advancing and receding contact angles are the maximum and minimum contact angles that caused by local surface defects. The equilibrium contact angle can be calculated from the advancing and receding contact angles (Tadmor, 2004).

The contact angle can be measured by the experiment such as sessile drop technique in Goniometer. It also can be calculated from the Young's equation (Eq.

2.6) which is the relationship between the contact angle and surface tensions. There are three surface tensions acting in equilibrium on a drop of liquid in the vapor phase on the solid as shown in Figure 2.2.

$$\sigma_{VS} - \sigma_{LS} = \sigma_{LV} \cos \theta \quad (2.6)$$

where, σ_{VS} , σ_{LS} , σ_{LV} , and θ are the surface tension at the interface of the vapor and solid phases, at the interface of the liquid and solid phases and at the interface of the liquid and vapor phases and the contact angle, respectively.

If the liquid drop completely spread on the solid surface, the contact angle is 0° . When the contact angle of water on the surface is smaller than 90° , the surface is considered hydrophilic, while the surface with the larger than 90° of water contact angle is hydrophobic. Some material surfaces, which have contact angles greater than 150° , are called superhydrophobic surfaces.

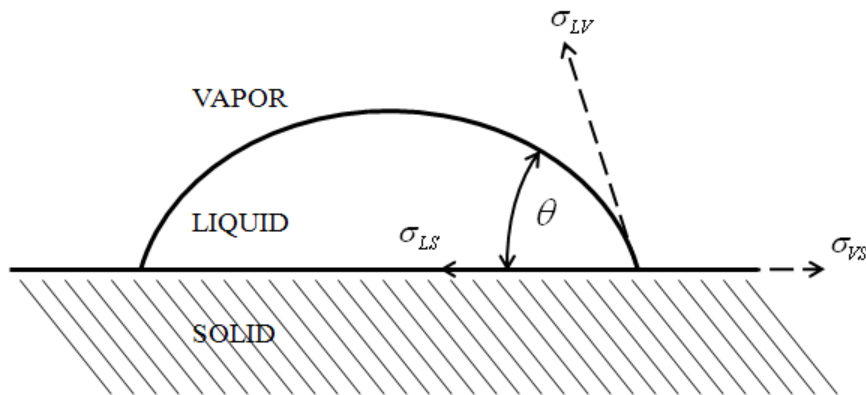


Figure 2.2 A sessile drop with contact angle and surface tensions

For water-organic system, the contact angle can be calculated from the Young's equations of air-water, air-organic and water-organic interfaces as shown below:

$$\sigma_{AS} - \sigma_{WS} = \sigma_{WA} \cos \theta_{WA} \quad (2.7)$$

$$\sigma_{AS} - \sigma_{OS} = \sigma_{OA} \cos \theta_{OA} \quad (2.8)$$

$$\sigma_{WS} - \sigma_{OS} = \sigma_{OW} \cos \theta_{OW} \quad (2.9)$$

where, the subscripts S, A, W and O correspond to solid surface, air, water and organic, respectively.

From these equations, the contact angle of organic in water phase (θ_{OW}) can be obtained from:

$$\sigma_{OW} \cos \theta_{OW} = \sigma_{OA} \cos \theta_{OA} - \sigma_{WA} \cos \theta_{WA} \quad (2.10)$$

The contact angle of water in organic phase (θ_{WO}) can be calculated by subtracting contact angle of organic in water phase by 180° .

In the two phase parallel flow in the microchannel, the position of the interface was fixed at the place that the ΔP_{Flow} and $\Delta P_{Laplace}$ are balanced (Aota et al., 2007). The ΔP_{Flow} can be estimated from the pressure loss toward the outlet. For a sufficiently narrow tube (low Bond number), the $\Delta P_{Laplace}$ is a result of the interfacial tension between phases and can be calculated from Young-Laplace equation written as follows:

$$\Delta P_{Laplace} = \frac{2\sigma \sin(\theta - 90^\circ)}{d} \quad (2.11)$$

where, d is the depth of the microchannel.

For the surface modification microchannel, the contact angles are limited to the values between the advancing contact angle of the aqueous phase on the hydrophobic surface in the organic phase θ_{WO} and that of the organic phase on the hydrophilic surface θ_{OW} in the aqueous phase. Therefore, $\Delta P_{Laplace}$ exist in the following range:

$$\frac{2\sigma \sin(\theta_{OW} - 90^\circ)}{d} < \Delta P_{Laplace} < \frac{2\sigma \sin(\theta_{WO} - 90^\circ)}{d} \quad (2.12)$$

For flow in conduits, by assuming the pressure at the outlet is atmospheric pressure (P_{atm}), the pressure of each phase (P) can be evaluated from the pressure loss (ΔP) as follows:

$$P = P_{atm} + \Delta P = P_{atm} + 2f\rho v^2 L / d_H \quad (2.13)$$

where f , v , and L are the friction factor, the mean velocity of the fluid, and the channel length.

For laminar flow, f is expressed as:

$$f = 16 / \text{Re} = 16\mu / \rho v d_H \quad (2.14)$$

Therefore, ΔP_{Flow} can be expressed as:

$$\Delta P_{Flow} = P_W - P_O = \frac{32\mu_W v_W L_W}{d_{HW}^2} - \frac{32\mu_O v_O L_O}{d_{HO}^2} \quad (2.15)$$

The interface can be fixed at the boundary between the hydrophilic and hydrophobic surfaces when ΔP_{Flow} is in the range of $\Delta P_{Laplace}$. On the other hand, the leakage occurs when the ΔP_{Flow} exceeds the $\Delta P_{Laplace}$ range.

Flow visualization in microchannels is challenging because of the optical resolution and refraction effects. The common methods are Laser induced fluorescence (LIF), confocal lasers scanning microscopy (LSM) and μ -PIV (Fries and Rudolf von Rohr, 2009a). Several methods with applications were reviewed by Sinton (2004).

2.3 CFD

Computational fluid dynamics (CFD) is the analysis of systems involving fluid flow, heat transfer and associated phenomena such as chemical reactions by means of computer-based simulation. Numerical method is applied to solve the partial differential equation system of the fluid dynamics by computer programming. There are many advantages of CFD over experiment approaches such as the ability to study

the systems that are impossible to perform or difficult to control the experiment and the ability to study the systems under hazardous conditions. In Engineering, using CFD can reduce cost and time to design and improve product. Nowadays CFD are being used increasingly in a wide range of application areas by researchers, equipment designers, and process engineers to analyze the flow and performance of process equipment.

Many commercial CFD software codes are available. The finite volume method is a numerical solution technique that is central to the most well-established CFD codes (Versteeg and Malalasekera, 2007) and FLUENT is one of the commercial finite volume codes.

There are three main components for all CFD codes, i) Pre-processor, ii) Solver and iii) Post-processor.

i) Pre-processor contains definition of the domain which is the geometry of the interested region, grid generation, physical and chemical phenomena selection, definition of fluid properties and boundary condition specification. Both the accuracy of a solution and its cost in terms of necessary computer hardware and calculation time are dependent on the fineness of the grid.

ii) In the solver part, partial differential equations are arranged and discretised to algebraic equations. These equations are solved by numerical methods. For FLUENT, finite volume method is applied for discretisation and iterative method is the numerical method means (Fluent Inc., 2006).

iii) For post-processor, the simulation results are displayed in different appropriate visualization tools to analyze the results.

Most of verification and analysis of CFD results are compared with some points of the problem to the experimental results or compared to other problems which are similar to the interested problem.

In the finite volume method, the domain is divided into discrete control volumes. The governing equations are integrated over a control volume to yield discretised equations. The property values are stored at the nodal point which is located at the center of each control volume. These property values are interpolated to the control volume faces and the gradients are approximated in order to calculate the governing equations.

For immiscible fluids, there are several available methods to model free surface flows such as level set, volume of fluid (VOF), marker particle, Lattice Boltzmann and front tracking. VOF and level-set approaches belong to the most common implicit free-surface reconstruction methods, while, particularly, VOF is relatively simple to treat topological changes of the interface and is naturally conservative (Kashid et al., 2008).

Volume of fluid method (VOF) is a surface tracking technique designed for multiphase fluids which the position of the interface between the fluids is of interest. VOF technique is widely used in commercial CFD codes and was first introduced by Hirt and Nichols (1982). The VOF model is based on the volume fraction field. In this method, a single set of momentum equations is solved and tracking the volume fraction of each of the fluids throughout the domain. The fluids are assumed to share the same momentum equation hence this method is not suitable for the cases which the fluid velocities are different significantly. The flow is considered Newtonian, so the momentum equation can be expressed in the Navier-Stokes equation as the following form:

$$\frac{\partial}{\partial t}(\rho \bar{v}) + \nabla \cdot (\rho \bar{v} \bar{v}) = -\nabla p + \nabla \cdot [\mu (\nabla \bar{v} + \nabla \bar{v}^T)] + \rho \bar{g} + \bar{F} \quad (2.16)$$

In Eq. 2.16, the accumulation and convective momentum terms in every control volume on the left-hand side balance the pressure force, shear force, gravity force and additional surface tension force \bar{F} on the right-hand side. ρ and μ are the physical properties that are average density and viscosity respectively which are

calculated by averaging based on the volume fraction of the individual fluid in each control volume. Therefore, the properties in a two-phase system can be written as:

$$\rho = \alpha_2 \rho_2 + (1 - \alpha_2) \rho_1 \quad (2.17)$$

$$\mu = \alpha_2 \mu_2 + (1 - \alpha_2) \mu_1 \quad (2.18)$$

and for n -phase system, for instance, q^{th} phase properties can be written as:

$$\rho = \sum \alpha_q \rho_q \quad (2.19)$$

where α is the volume fraction and the subscripts represent the phases.

The equation for conservation of mass or continuity equation can be written as follows:

$$\frac{\partial \rho}{\partial t} + \nabla \cdot (\rho \bar{v}) = S_m \quad (2.20)$$

where S_m is the added mass source.

In FLUENT, the tracking of the interface between the phases is accomplished by the solution of a continuity equation for the volume fraction of one phase. For the q^{th} phase, this equation can be expressed as:

$$\frac{1}{\rho_q} \left[\frac{\partial}{\partial t} (\alpha_q \rho_q) + \nabla \cdot (\alpha_q \rho_q \bar{v}_q) \right] = S_{\alpha_q} + \sum_{p=1}^n (\dot{m}_{pq} - \dot{m}_{qp}) \quad (2.21)$$

where \dot{m}_{pq} is the mass transfer from phase p to phase q and \dot{m}_{qp} is the mass transfer from phase q to phase p. The source term, S_{α_q} , is zero by default but can be specified as a constant or user-defined mass source for each phase.

The primary-phase volume fraction will be computed based on the following constraint:

$$\sum_{q=1}^n \alpha_q = 1 \quad (2.22)$$

In order to add the surface tension effect to the VOF calculation, the continuum surface force (CSF) model proposed by Brackbill et al. (1992) is surface tension model in FLUENT. The calculated surface tension force is added as a source term in the momentum equation. For two phases, a source term can be written as follows:

$$F_{vol} = \sigma_{ij} \frac{\rho \kappa_i \nabla \alpha_i}{\frac{1}{2}(\rho_i + \rho_j)} \quad (2.23)$$

where κ is the curvature computed from the divergence of the unit surface normal:

$$\kappa = \nabla \cdot \hat{n} \quad (2.24)$$

where

$$\hat{n} = \frac{n}{|n|} \quad (2.25)$$

and the surface normal defined as the gradient of the volume fraction of the q^{th} phase.

$$n = \nabla \alpha_q \quad (2.26)$$

Despite being successful in computing the surface tension effects, one major remain limitation is to introduce spurious ‘parasitic’ currents in form of low magnitude velocity fields around the region of the interface especially when the curvature is high. This may be reduced by applying a more accurate estimation for the curvature (Meier et al., 2002). In addition, it is also dependent on the grid density. Thus, the refined mesh at the interface location should be able to improve these approximations (Balachandran, 2009).

The importance of surface tension effects is determined by the value of the dimensionless quantities. In the case of $Re \ll 1$, the quantity of interest is the capillary number and the surface tension effects can be neglected if $Ca \gg 1$. For $Re \gg 1$, the quantity of interest is the Weber number and the surface tension effects can be neglected when $We \gg 1$ (Fluent Inc., 2006).

For wall adhesion effect, the surface normal in cells near the wall is corrected by the contact angle. The surface normal at the cell next to the wall can be expressed as:

$$\hat{n} = \hat{n}_w \cos \theta + \hat{t}_w \sin \theta \quad (2.27)$$

where \hat{n}_w and \hat{t}_w are the unit vectors normal and tangential to the wall, respectively.

These equations are solved iteratively under appropriate initial and boundary conditions.

CHAPTER III

LITERATURE REVIEWS

In this chapter, the literature reviews involving multiphase flow and simulation in microreactor are provided. It is divided into three sub-topics. Firstly, previous works on flow patterns of two-phase fluids in microreactor are presented. Next, the liquid multiphase parallel flow is highlighted and the stabilization method in microreactor is reviewed. Then, the CFD simulation of multiphase flow in microreactor is summarized. Finally, the multiphase flow in small curved channel study is reviewed.

3.1 Two-phase flow pattern

Many investigations of liquid-liquid two-phase flow have been conducted in a wide range of experimental conditions and a variety of flow patterns have been reported. The multiphase flow pattern dependence on the flow rates study is usually constructed as flow regime or flow pattern maps. The flow pattern boundaries in the map are not distinct and the transition can be rather unpredictable since they may depend on otherwise minor features, such as wall roughness or entrance conditions (Brennen, 2005). Lin and Tavlarides (2009) summarizes experimental investigations of oil-water two-phase flow patterns since 1996. Figures 3.1 and 3.2 show the flow patterns observed for liquid-liquid two-phase flow in vertical and horizontal pipes.

For liquid-liquid flow in small channel, Beretta et al. (1997) investigated the patterns of oil-water flow in glass Y-junction tubes with the test section of approximately 3 mm in diameter. Five types of flow patterns were shown by visual study, dispersed flow, slug flow, bubbly flow, plug flow and annular flow which are suggested to classify into three regimes, dispersed (dispersed flow), intermittent (slug, bubbly and plug flows), annular (annular flow). Brauner (1990) reported theory and experimental results seem to match each other quite well.

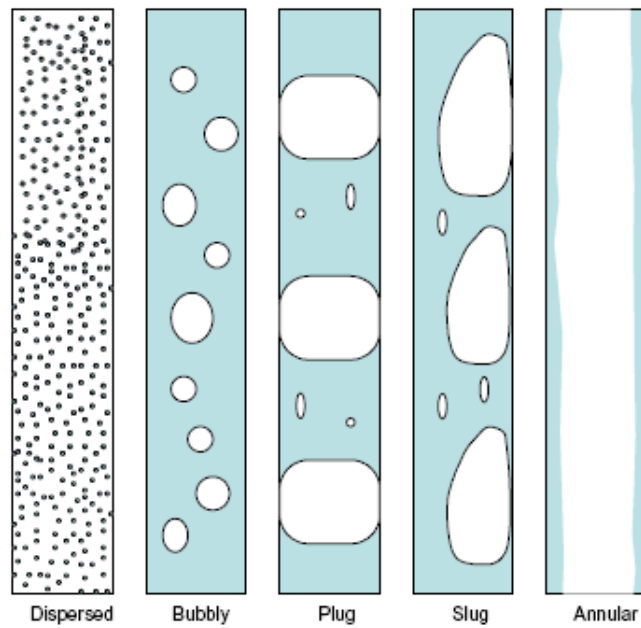


Figure 3.1 Flow patterns of liquid-liquid two-phase vertical upward flow in pipes
(Lin and Tavlarides, 2009)

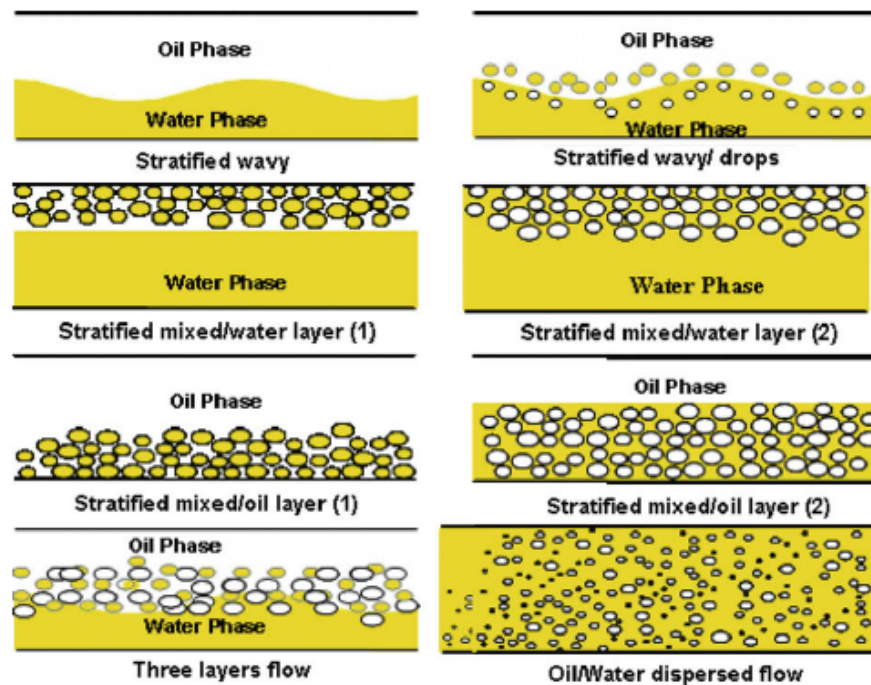


Figure 3.2 Observed oil-water flow patterns in a horizontal 0.0254 m pipe
(Al-Yaari et al., 2010)

In microreactor, the multiphase flow patterns are difficult to predict and control due to dependence on many experimental parameters which must be considered simultaneously (Dessimoz et al., 2008). The multiphase flow patterns and the transfer processes in microreactors have been investigated recently by many researchers and particular focus was on gas-liquid systems. The flow pattern of gas-liquid in microchannels generally has been classified into four different flow regimes, stratified, bubbly, annular, and intermittent flow patterns (Weinmueller et al., 2009, Chen et al., 2009). Table 3.2 shows the classified regimes and subdivided flow patterns and Figure 3.3 shows the experimental images of these flow patterns. The liquid-liquid system has received less interest and still less understood than gas-liquid system (Angeli and Hewitt, 2000, Burns and Ramshaw, 2001, Zhao et al., 2006, Lin and Tavlarides, 2009).

Table 3.2 Gas-liquid flow pattern in microchannels (Weinmueller et al., 2009)

<i>Major flow regime</i>	<i>Flow pattern</i>
Dispersed	Dispersed bubbly
	Regularly ordered bubbly
Intermittent (Taylor)	Wedging (elongated bubbly, plug)
	Slug flow
Annular	Smooth annular
	Wavy annular
Stratified	Smooth stratified
	Wavy stratified

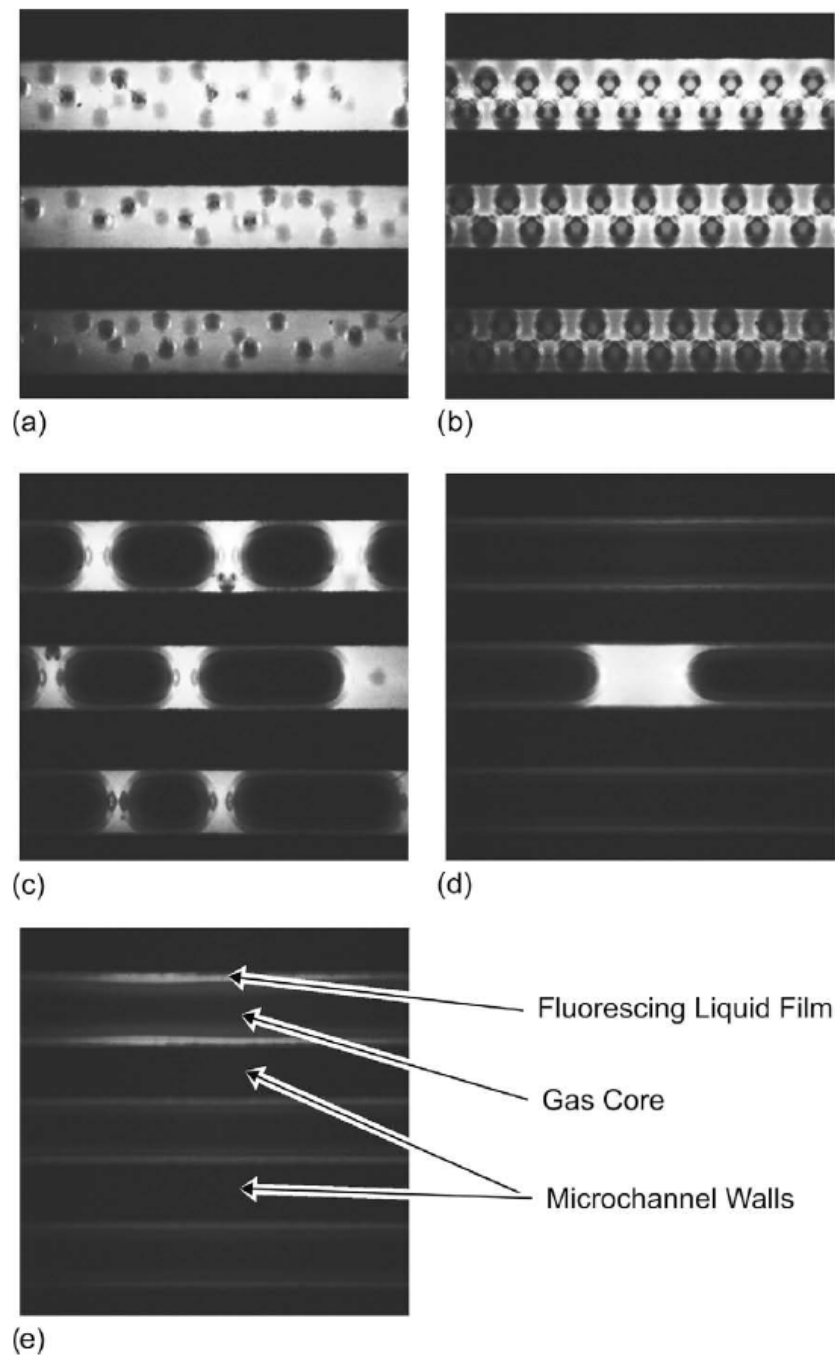


Figure 3.3 Micro-PIV images from: (a) bubbly, (b) regularly ordered bubbly flow, (c) wedging, (d) slug, and (e) annular flow (Weinmueller et al., 2009)

For liquid-liquid two-phase flow in microreactors, droplet, slug, stratified (or parallel) and annular flow have been reported in many works. Figures 3.4 and 3.5 illustrate the liquid-liquid two-phase flow patterns observed in microchannels. Many parameters that affect on these flow patterns have been studied.

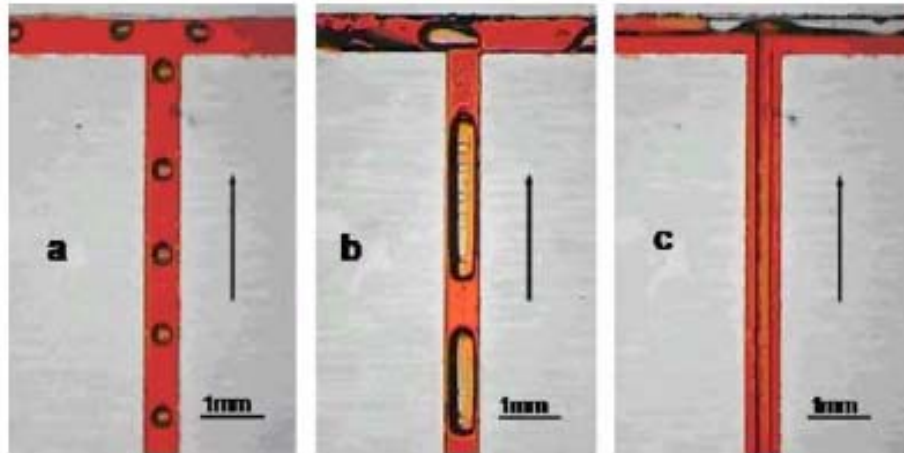


Figure 3.4 Photographs of oil-water flow patterns in microchannel initially saturated with oil: (a) droplet flow, (b) slug flow, and (c) annular flow (the arrow indicates the flow direction) (Salim et al., 2008)



Figure 3.5 Snapshot of parallel flows that have smooth interface in microchannel (Zhao et al., 2006)

Flow rate and ratio effects were investigated and plotted as the flow pattern maps in many different specific systems (Dreyfus et al., 2003, Zhao et al., 2006, Kashid et al. 2011). Figure 3.6 shows the liquid-liquid flow pattern map for different literature data.

The flow behavior also depends on the microchannel types such as T- and Y-junction contactors (Kashid and Kiwi-Minsker, 2009). Kashid et al. (2011) examined the water-toluene flow pattern in five different microchannels (both types of mixing junctions in combination with the cross section geometries). Six different flow regimes which are slug, slug-drop, deformed interface, parallel/annular, slug-

dispersed, and dispersed flow were observed. The results showed that no significant effect of the microchannel cross section on the flow regimes.

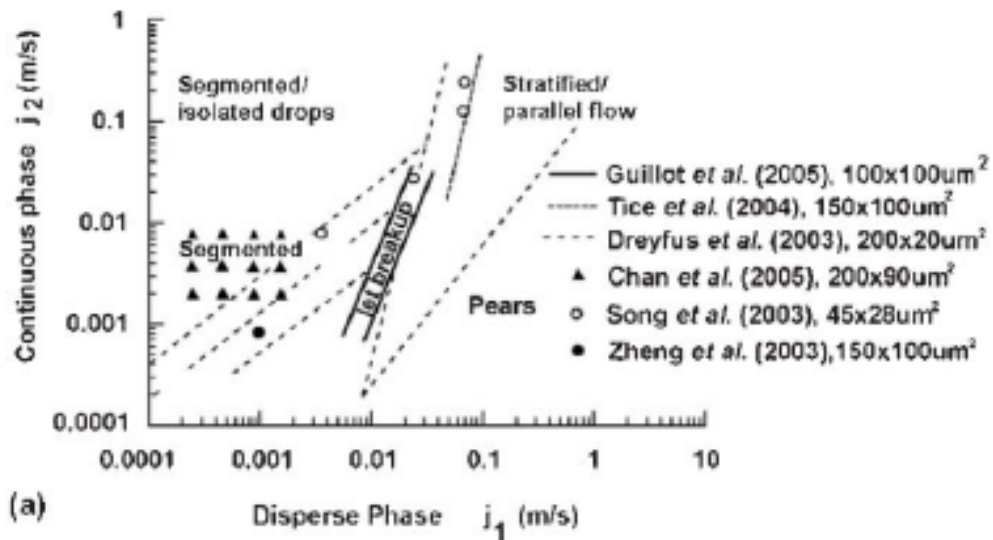


Figure 3.6 Liquid–liquid flow patterns in microfabricated systems diagram with transition lines and operating conditions for different literature data (Günther and Jensen, 2006)

The effect of fluid properties on the flow characteristic has been studied. Dessimoz et al. (2008) studied the influence of the fluid properties by adding solutes in both phases in order to change the density, the viscosity and the interfacial tension of the fluid system. In the test water-toluene system, an increase of the interfacial tension in comparison to viscous forces by adding sodium hydroxide was favorable for slug flow and a decrease of the interfacial tension in comparison to viscous forces by trichloroacetic acid resulted in parallel flow.

The surface properties affect the contact angle and the flow pattern. The effect of surface wettability in water-kerosene flow system was investigated by Zhao et al. (2010). The contact angle of Polymethylmethacrylate (PMMA) microreactor was changed after surface modification and the fluctuation amplitude is larger than before surface modification at the opposed T-junction.

For the initial fluid, different flow patterns have been observed depending on the nature of the first fluid injected into the microchannel. Salim et al. (2008) investigated the flow pattern with different first fluid injected in glass and quartz microchannels. From the contact angle measurement, oil is more wetting than water for both materials. In the same microchannels, the observed flow configurations were different as the first fluid changed. With the same first fluid injected, quartz and glass provide the same patterns when the microchannels were initially saturated with oil but different patterns when the microchannels were initially saturated with water.

3.2 Parallel flow stabilization in microreactor

The general patterns of liquid-liquid two-phase flow are slug flow and parallel flow. In the slug flow pattern, mass transfer between two phases occurs by two mechanisms that are molecular diffusion due to concentration gradients between adjacent slugs and convection due to the internal circulation in each slug (Burns and Ramshaw, 2001, 2002, Dumann et al., 2003, Kashid et al., 2005). This circulation is a result of shearing action between the slug axis and the continuous phase or wall axis. This fluid motion enhances mixing within the segments and also improves the rate of diffusion across the interface by the shearing disturbance of concentration gradients within the segments. For parallel flow pattern, the flow is laminar and the mass transfer between the two fluids occurs only due to molecular diffusion. Although parallel flow pattern provides relatively low interfacial area and mass transfer compared to slug flow, a phase separation at the exit of microreactor is available.

In a practical point of view, a stable multiphase laminar flow in microchannel can provide a phase separation of the product mixture and then reduces the post-treatment unit operations requirements. This phase separation is important in the continuous flow microsystem design. Hibara et al. (2001) demonstrated that quite stable multilayer flow can be formed in a microchannel. The results were explained that the contribution of gravity can be neglected compared to the interfacial tension with 100 μm order scale.

Many techniques have been proposed to stabilize the parallel flow pattern such as incorporating a surfactant (Reddy et al., 2005, Aljbour et al., 2009a), introducing membrane (Hisamoto et al., 2003, Kralj et al., 2007), adding guideline structure (Surmeian et al., 2002, Tokeshi et al., 2002, Maruyama et al., 2004, Tagawa et al., 2007) and modifying the microreactor surface (Hibara et al., 2002, 2005, Maruyama et al., 2003, Smirnova et al., 2006, Yamasaki et al., 2009).

The surfactant is added to reduce the interfacial tension between the two immiscible liquid phases. A typical surfactant molecule has a hydrophilic head which immerses in the aqueous phase and hydrophobic tail resides in the nonpolar phase. There is a critical concentration of surfactant, known as the critical micellar concentration (CMC). The surfactant molecules are mostly at the interface of the fluid at concentrations lower than the CMC. When the surfactant concentration exceeds this value, surfactant molecules organize themselves into micelles (Baroud and Willaime, 2004).

A guideline structure can stabilize a parallel flow by reducing the contact area between the flowing phases. As a result of the confined space, the interfacial force is reduced and the fluid minimizes itself to keep a minimum interfacial energy. In addition, the viscous force is also increased as a result of the increased phase velocity in smaller confinements (Aljbour et al., 2009b). There were two types of guide structure have been used, continuous and intermittent. For application, two and three guided layer flows have been studied.

To maximize the specific interface area and stabilize the liquid-liquid interface, Tokeshi et al. (2002) used the microchannels with the lowest height continuous guide structures that can form the stable interface at the operate condition to study a new design of continuous flow Co(II) wet analysis. With these guide structures, the phase separation was possible.

Maruyama et al. (2004) studied liquid-liquid extraction of metal ions in a microreactor with the same wall and gap length intermittent partition walls in the center. There was no stable two phase flow achieved in the microchannel with the

longer wall length than 100 μm at the fixed aqueous flow rate. The structure allowed clear phase separation compared to without walls. The partition walls were induced a slight turbulence which promoted the transport of the ions. 2D CFD simulation was also done by volume of fluid (VOF) method using Fluent 5.5. The simulation result agreed with the flow visualization experiment.

Tagawa et al. (2007) tested the stability and phase separation of equal flow rate toluene and water two-phase flow in a microchannel with an intermittent guideline structure. Flow rates larger than 0.02 ml/min exhibited a stable two-phase laminar flow for model TSR35. In stable flow, toluene was not detected in the aqueous phase and only a small amount of water was detected in the organic phase when the sum of feed flows is higher than 0.050 ml/min. Furthermore, the reduction of the mass transfer limitations in microreactors was exhibited by conducting the hydrolysis reaction of benzoyl chloride. The conversions were much higher when compared with batch reactor at the same space-time.

In 2008, Aljbour et al. conducted the tri-liquid phase ethoxylation with a phase transfer catalyst in a microchannel with a continuous guideline structure. The structure guided the flow and minimized the interfacial instability that might lead to the disappearance or dispersion of the third catalytic phase. The computed apparent rate constant in the microchannel reactor was several orders of magnitude higher than the batch reactor with different speeds of agitation even at lower temperature. In 2009, they investigated the phase transfer catalyzed reaction in the continuous guided microchannel reactor. The parallel multiphase flow was formed at equal phase flow rates larger than 0.007 ml/min. The organic phase was separated completely when the total feed flow rate is higher than 0.02 ml/min but the whole aqueous phase was impossible to separate from the aqueous phase outlet due to the wettability. With time, the byproducts are accumulated. These salts cause the switching from parallel to slug flow and retarded the reaction but it was removed completely by using acid.

For surface modification technique, there are both increasing hydrophobicity and hydrophilicity cases. In the first case, generally hydrophilic nature surface of organic phase channel wall is changed to be hydrophobic by silanization (or

silanation). The surface silanol groups are replaced with silane functional groups. The silanization mechanism starts with the physisorption of the chlorosilane group on the adsorbed water layer on the substrate followed by the hydrolysis of trichlorosilanes to form trisilinsols. After that, there is condensation to form the covalent siloxane bond at the substrate surface. Finally, the cross-linking between the adjacent silanols occurs to stabilize the film (Brzoska et al., 1994).

Flinn et al. (1994) characterized silica surfaces modified by using octadecyltrichlorosilane (OTS) as a silane agent. The OTS molecules form small patches on the surface. The OTS film stability and uniformity was controlled mainly on the amount of water in the system. The stability of the organic-aqueous interface was clearly improved and the flexible flow rate ratio was possible by surface modification using octadecylsilane (ODS) in the glass microchip (Hibara et al., 2002, 2005). Besides silica and glass materials, silanization was also applied on mica (Carson and Granick, 1990) and alumina (Rosu and Schumpe, 2010).

For the latter case, the Polymethylmethacrylate (PMMA) hydrophobic nature could be changed to hydrophilic by coating with TiO_2 layer and the modified microchannel provided the stable layered flow (Yamasaki et al., 2009). The PMMA surface was also successfully changed by modifying with sodium hydroxide and alumina hydroxide sol (Zhao et al., 2006, 2010) and Plasma treatment (Chai et al., 2004, Reichen et al., 2009). A stainless steel microchannel could modify by silicon sol (Zhao et al., 2010) to increase the surface wettability.

Aljbour et al. (2010) examined the effect of surface modification on the performance of phase separation in a glass microreactor with continuous guideline structure. After silanization with octadecyltrichlorosilane (OTS), each phase was confined within its corresponding channel and an aqueous phase film surrounded the organic phase was disappeared. By adjusting the organic-to-aqueous flow rate ratio at the fixed organic phase flow rate at 0.18 ml/min, the ratio around two provided the acceptable phase separation.

3.3 CFD application in multiphase microreactor

CFD method has been applied to study the hydrodynamic of multiphase system in micro-scale. Both 2D and 3D (two and three-dimensional) spaces have been used.

Various researchers applied CFD on the slug flow (Harries et al, 2003, Kashid et al., 2005) because it can provide detailed flow field information. Harries et al. (2003) developed a numerical model based on CFD for segmented flow in a microreactor to predict the internal flow patterns and the transfer of dissolved chemical species. Segmented flow was approximated by two adjacent rectangular units in a microchannel with no-slip condition moving walls. Both phases were incompressible and Newtonian with equal viscosity. The calculated vector map exhibited the vortex flow patterns in the segments. By implementing acid/base reaction, concentration maps representing the distribution of acetic acid as it diffuses and partitions across the interface were shown. Mass transfer and the flow pattern were well predicted. Segment length depended on flow rate and fluid properties.

Kashid et al. (2007b) developed a finite element based CFD model to study the flow patterns within the slugs and mass transfer with and without chemical reaction. The model was similar to Harries et al. (2003) but accounted for the effect of viscosity. From the velocity vector plot, higher viscosity fluid took more time to reach steady-state but the steady-state profiles were similar and thus not affected on the mass transfer performance. The extraction of succinic acid from aqueous solution with *n*-butanol was simulated for mass transfer. For different refinement levels, the concentration and mass transfer coefficient curve showed a slight difference at saturation point but showed a significant difference before saturation. The titration reaction was simulated and the results were in good agreement with experimental and numerical results of Harries et al. (2003) but slightly higher at low velocity. Some reasons for the difference might be the assumption of flat interface and the wall film existence. In 2008, Kashid et al. discussed the hydrodynamics of the liquid-liquid slug flow in 120° Y-junction microreactor using experimental and computational techniques. VOF approach by FLUENT and level-set approach by FEATFLOW

showed the well-defined slug flow. Particle imaging velocimetry (PIV) measurements and FEATFLOW free-surface modeling were used to exhibit the internal circulations and interface behavior. The particle-tracing technique was also applied for flow field visualization. Simplified modelling-single phase assuming the fixed interface position retrieved from the experimental snapshots also showed very good results.

Glatzel et al. (2008) studied the performance of four CFD software programs, CFD-ACE+, CFX, Flow-3D and FLUENT by simulating four different microfluidic applications in 3D. The free surfaces were treated by the volume of fluid (VOF) method and flow patterning was visualized with a scalar marker method. The consistency of results, computational speed and comparison with available experimental data were used to evaluate the different program simulation results. Generally CFD-ACE+ and Fluent can be recommended for simulation of free surface flows involving capillary forces.

FLUENT is well-known commercial software used to study in a number of research works. Qian and Lawal (2006) applied FLUENT to investigate gas-liquid slug flow in the microchannel. The effects of many parameters on the slug size were studied. The accuracy of VOF model in the FLUENT to represent a real surface was verified by Balachandran (2009). The thin liquid film flowing into a cavity with the shearing air flow was simulated with the geometric reconstruction scheme both small and large surface tensions. The validity was analyzed by using the fact that the normal velocity of the interface must be zero at a steady state condition. When the value of surface tension increases, the interface becomes flatter as expected. The normal velocities were calculated on the assumed interface which located at water volume fraction equals to 0.5. As surface tension increased, there was more non-zero normal velocity which confirmed the presence of parasitic current in VOF model in the Meier et al. (2002) results.

3.4 Multiphase flow in small curved channel

In common, a long channel is designed as serpentine configuration confined in the available space to increase the flow length or residence time for given flow rates. The mixing performance was enhanced by a secondary or Dean flow induced by centrifugal force in a single phase system. For multiphase system, the effects of channel material and aspect ratio on the liquid-liquid slug flow in serpentine minichannels were examined by Kulkarni and Kalyani (2009). In PMMA channel, the small aspect ratio shows strong effects of inlet flow rate and flow rate ratio on the slug size distribution, while there is no specific slug size distribution trend observed in a larger aspect ratio channel. Vashisth and Nigam (2009) studied the stratified gas-liquid flow in coiled tube using CFD method. The 3D model was simulated in FLUENT 6.2 using volume of fluid (VOF) approach. The result shows the shifting of the maximum velocity towards the coiled tube outer wall because of the unbalanced centrifugal forces. The effects of gas and liquid velocity, pitch and curvature ratio on the flow were investigated.

In micro-scale, the gas-liquid slug flow in curved channel has been studied by CFD method and experimental visualization. Kumar et al. (2007) simulated the 3D model in FLUENT 6.3 to investigate gas and liquid development in curved microchannel with different inlet geometries. The volume of fluid (VOF) was used to track the interface. With the single inlet model, the observed flow reversal phenomenon at the entrance of curved section was disappeared and the slug length was increased when the curvature ratio was increased. This may be due to the increasing curvature ratio decrease the centrifugal force. The slug is generally stable with non-uniform length. The slug lengths are different due to the difference of the inlet configuration. Fries et al. (2008) used micronresolution particle image velocimetry (μ -PIV) to analyze liquid flow distribution. The effects of velocities, diameter and curve radii on the hydrodynamics and the liquid slug elongation were discussed. Some design rules were proposed base on the results to increase the recirculation and the expected mass transfer in the gas-liquid slug flow in curved microchannel.

For parallel flow in curved microchannel, the miscible liquid system was examined by Yamaguchi et al. (2004). The effects of velocity and curvature radius on the interface were demonstrated using both 3D CFD and experiment. The secondary flow induced by the centrifugal force affected the interface shape and the interface area could be increased. Base on diffusion, this increased area could promote a mass transfer across the interface.

CHAPTER IV

NUMERICAL MODELLING

In this chapter, multiphase flows in microreactors were simulated using the commercial software, FLUENT, in 2D and 3D. Before our problem simulations, the software was validated with the similar published problems to ensure its reliability. All problem solutions were obtained by following these six steps,

- a. Create geometry in GAMBIT
- b. Mesh geometry in GAMBIT
- c. Specify boundary types in GAMBIT
- d. Set up the problem in FLUENT
- e. Solve the problem in FLUENT
- f. Analyze the results

For all problems, simulations with refined grid were carried out to confirm that the solutions were grid resolution independent.

4.1 Commercial software validation

The accuracy of the commercial software, FLUENT, is considered first to make sure that the software is reliable by checking with the published problems. The qualitative and quantitative results from FLUENT software version 6.3 and 12.0 were compared with the reported experimental and simulation results.

4.1.1 2D parallel flow pattern

The FLUENT software version 6.3 was tested to simulate the two phase parallel flow in the microreactor as in the work of Huh et al. (2009). The 2D model geometry was created and meshed in GAMBIT software. The total cells were 58,000. The boundary types were specified in GAMBIT before the mesh was exported to FLUENT. Figure 4.1 shows the simulation model of three inlet microchannel. The upper and lower inlets are air inlets and the middle inlet is for water.

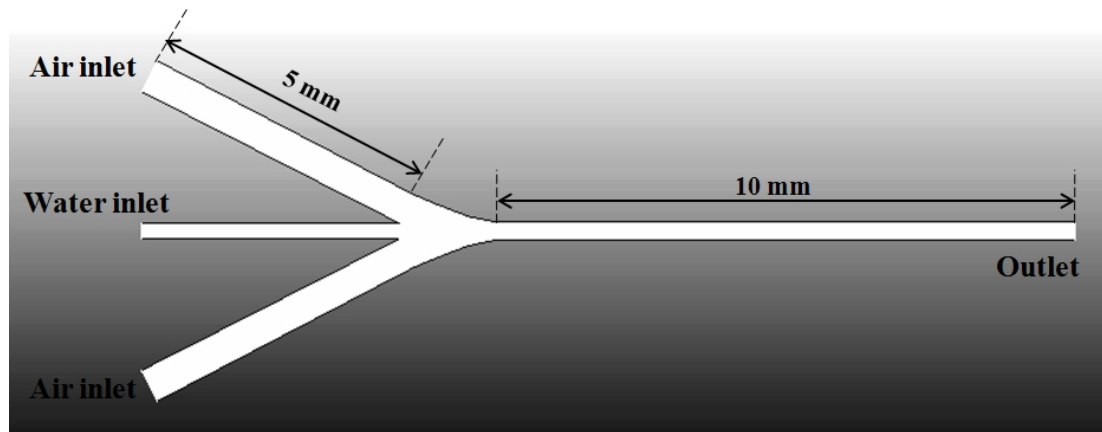


Figure 4.1 2D validation three inlet microchannel

The solver, material and phase properties were specified. The surface tension of water-air is 0.0728 N/m and the contact angle of water in air on untreated hydrophobic polydimethylsiloxane (PDMS) is 111° . The model was solved at the air and water superficial velocities of 20 and 0.4 m/s respectively. The simulated phase contour shows the stable stratified flow pattern similar to the experimental result. The simulated flow pattern in Figure 4.2 is in good agreement with the experimental flow image of this regime (Fig. 2 of Huh et al., 2009).



Figure 4.2 2D simulated stable stratified flow of the air (dark gray) and water (light gray) at superficial velocities of 20 and 0.4 m/s, respectively

4.1.2 2D slug size

The FLUENT software version 6.3 was also validated with the quantitative data. The two-phase Taylor flows were simulated in the 2D T-shaped microchannel model to compare with the results reported by Guo and Chen (2009). The model was created and meshed to 10,335 cells in GAMBIT. Air and water were used as gas and liquid phases, respectively. In the experiment, sodium dodecyl sulfate (SDS) was added to reduce the surface tension and improve wall wetting property. Therefore, the surface tension of water-air was specified at 0.031 N/m and the contact angle of water in air was set to 0° . Gas and liquid phase superficial velocities (U_G and U_L) were varied to investigate the effect on the gas slug size (L_G). Figure 4.3 shows the simulated slug flow pattern. The slug size was estimated as the length from tip to the other tip at the channel center as depicted by Fries and Rudolf von Rohr (2009b). The simulation results were in good agreement with both experimental and numerical results of the published work as shown in Figure 4.4.



Figure 4.3 2D simulated slug flow of air (dark gray) and water (light gray) at superficial velocities of 0.0694 and 0.0764 m/s, respectively

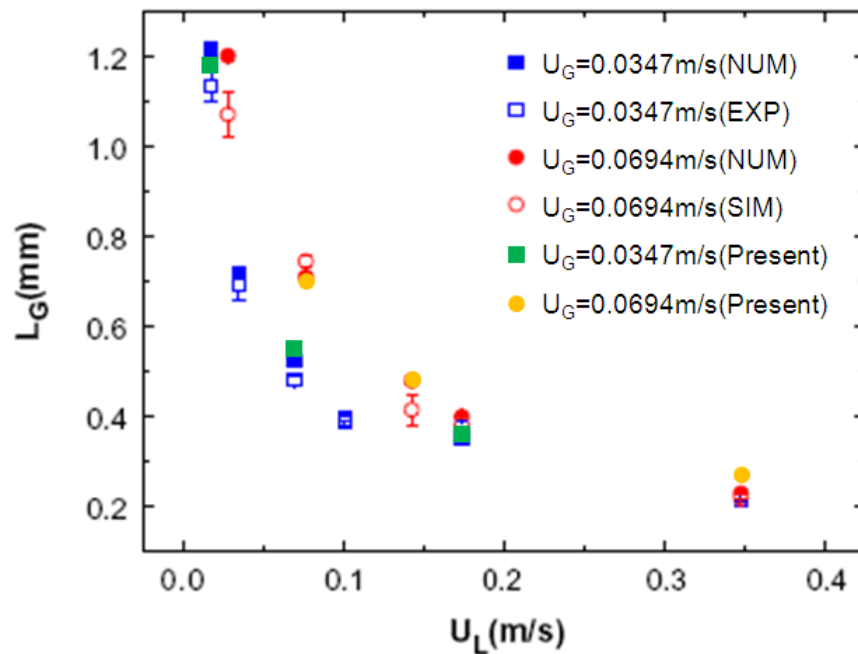


Figure 4.4 Comparison of the 2D slug length between the simulated results and the results reported by Guo and Chen (2009)

4.1.3 3D flow pattern and slug size

The FLUENT software version 12.0 was validated with the results published by Reddy Cherlo et al. (2010). Two phase liquid flows were simulated in the 3D T-shaped microchannel model which created and meshed in GAMBIT. The total cells are 156,000. The model with grids is shown in Figure 4.5. Water and kerosene were fed as aqueous and organic phases, respectively. The surface tension of water and kerosene is 0.045 N/m. The contact angle of kerosene in water on PMMA was calculated using Young's equation and obtained as 77.48° . The flow rates were varied to examine the effect on flow pattern and slug size. Figure 4.6 shows the simulated slug flow pattern. The simulated water slug lengths were compared with the experimental and 78° contact angle simulated results, which were approximated from Figure 4 in the work of Cherlo et al. (2010), as shown in Table 4.1.

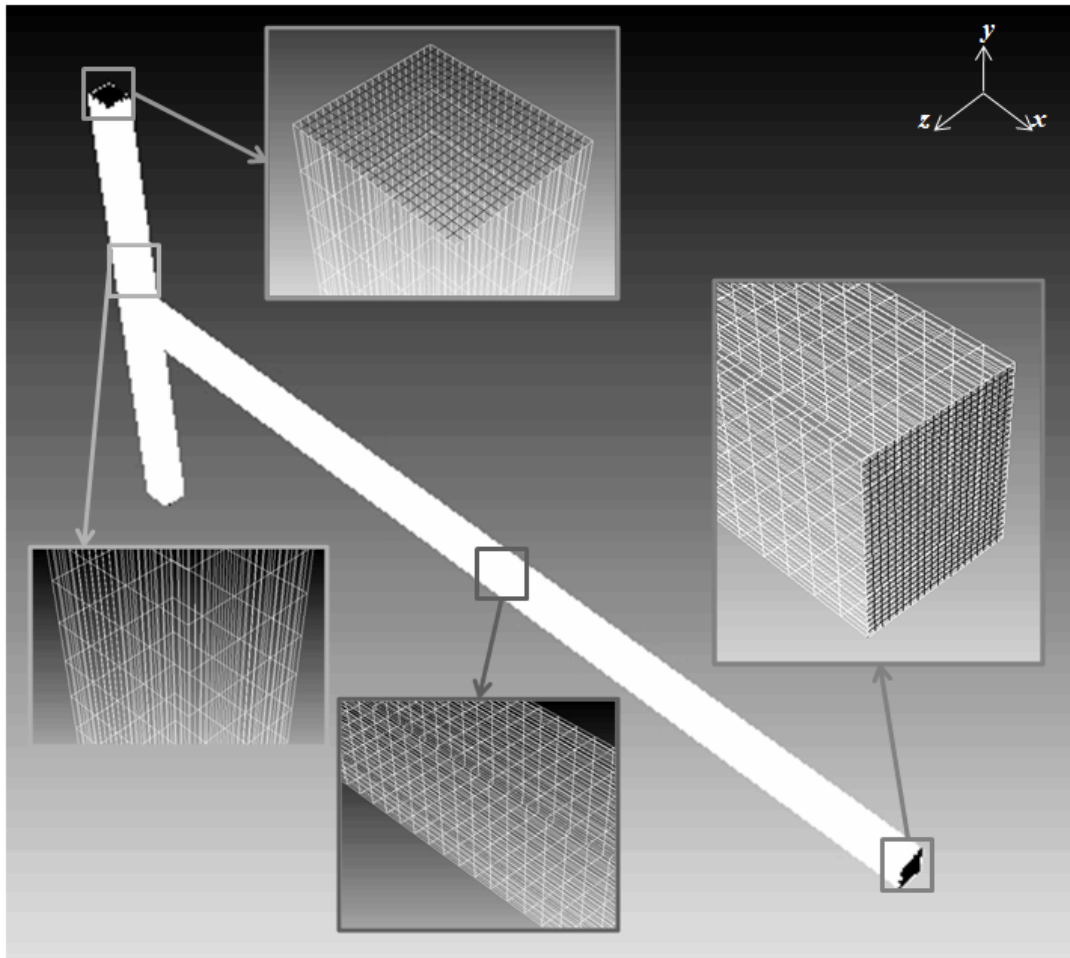


Figure 4.5 3D validation model with grids

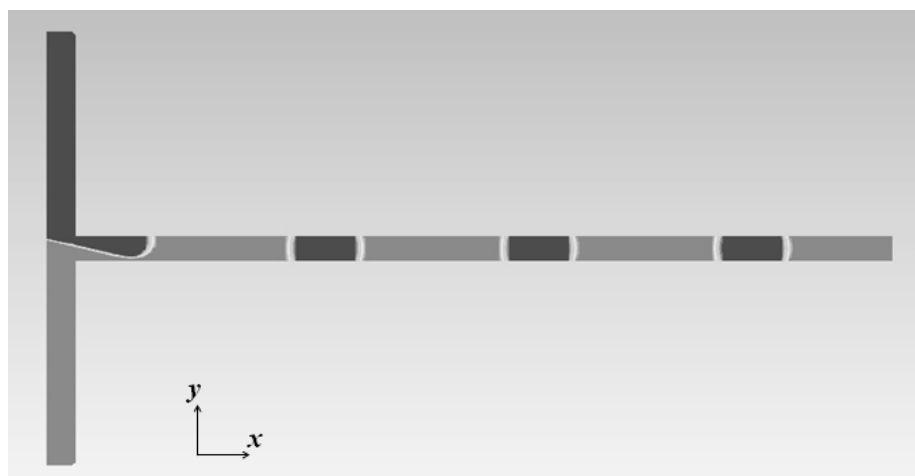
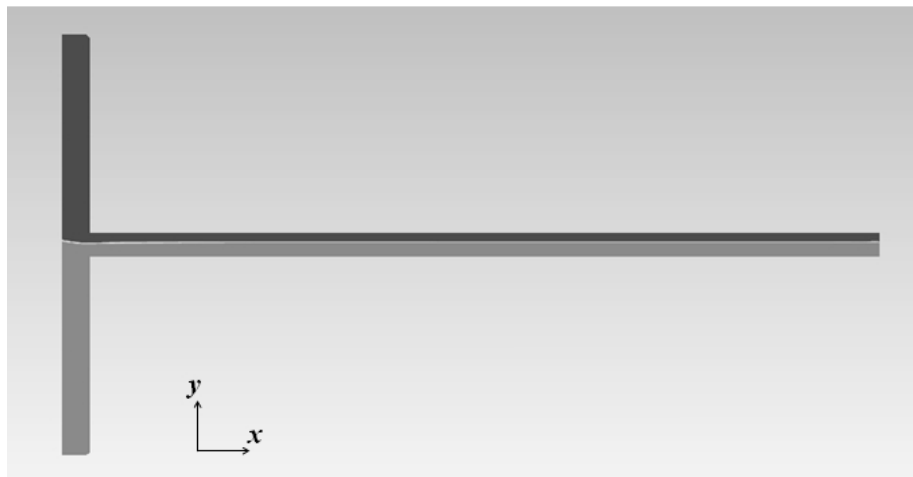


Figure 4.6 Simulated slug flows of water (dark gray) and kerosene (light gray) at flow rates of 10 and 20 ml/h, respectively

Table 4.1 3D validation water slug length

Water and kerosene flow rates (ml/h)	Water slug length (mm)		
	Experimental results	Published simulated results	Present simulated results
10 and 20	~2.05	~1.33	1.77
10 and 40	~1.6	~1.07	1.38

The simulation results at the equal fluid flow rates of 150 and 300 ml/h were parallel flow as shown in Figure 4.7. These are agreed with the experimental results shown in Figure 8 of the literature.

**Figure 4.7** Simulated parallel flows at each phase flow rates of 150 ml/h

4.2 Microreactor simulation

The research problems were simulated in 2D for the straight microchannel cases and in 3D for the curved microchannel cases.

4.2.1 2D straight microchannel

a. Create geometry in GAMBIT

The models of straight microchannel with two inlets as shown in Figure 4.8 were created in the pre-processor program called GAMBIT. From the figure, the inlets are on the left hand side and the upper one is water inlet while the other one is toluene inlet. The white dash line in the middle is guideline structures. Both liquid outlets which correspond with the inlets are on the right.

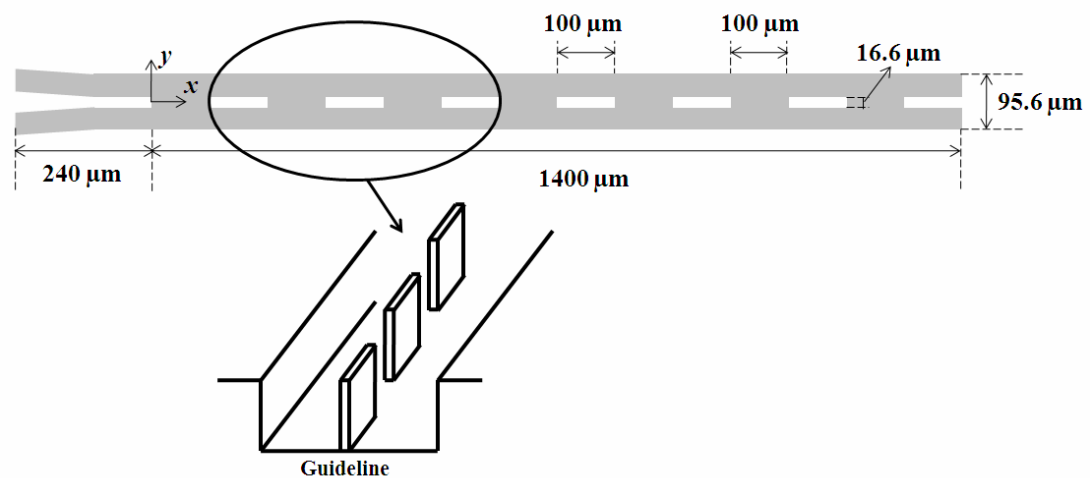


Figure 4.8 Microchannel with guideline structure (model A)

The effect of guideline was investigated by varying the guideline structure as summarized in Table 4.2. Experiments were conducted with the TSR13 microchannel sample represented by model A and reported by Tagawa et al. (2007).

Table 4.2 Guideline structure length

Model	Length (μm)	Interval (μm)
A	100	100
B	100	180
C (No guideline)	-	-

b. Mesh geometry in GAMBIT

The geometries were meshed as shown in Figure 4.9 by GAMBIT. The grid sizes in the x direction were 5.56 and 7.00 μm for the channel and the inlets, respectively. In the y direction, the maximum grid size was 2.51 μm and the minimum was 0.57 μm . The meshes were finer in the near guideline wall region and gradually increased in size towards the channel walls. With the same grid size, the total cells were 20,400 for model A, 20,600 for model B and 22560 for model C.

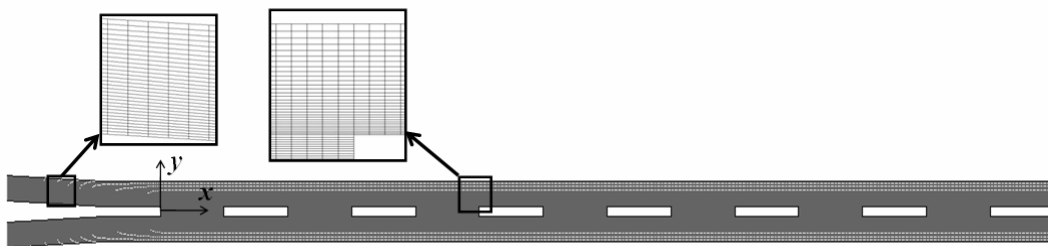


Figure 4.9 Microchannel model A with grids

c. Specify boundary types in GAMBIT

The boundary types were set in GAMBIT. The water and toluene inlets were defined as velocity inlet. The water and toluene outlets were specified as outflow. The rest edges were defined as wall type.

The effect of surface modification was investigated by comparing the unmodified case with the surface modified case. In the unmodified surface simulation case, the surface properties are the same for the whole surface (specified wall boundaries) of the microchannel. For the modified surface case, the surface was divided into two parts, organic and water, as shown in Figure 4.10. Thus the wall type edges were separated into two groups corresponding to the fluids, wall for water part and modified wall for organic part.

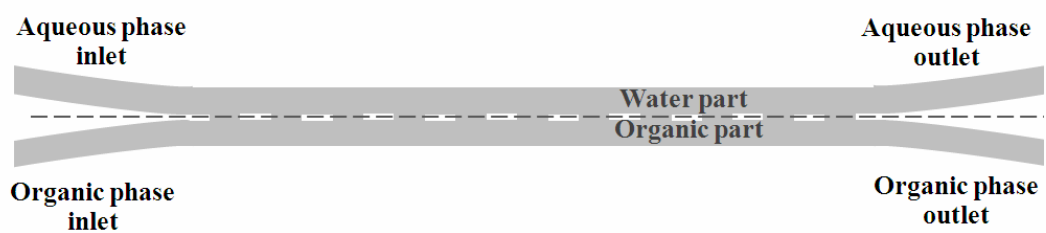


Figure 4.10 Water and organic parts in the modified surface microchannel

After specifying the boundary types, the meshes were saved and exported as the mesh type.

d. Set up the problem in FLUENT

The meshes were imported to FLUENT along with the boundary types specified. The models were scaled to millimeter. Then the pressure-based segregated solver which is suited for low-speed incompressible flow was used and the algorithm is shown in Figure 4.11. The implicit formulation, 2D space, transient flow and absolute velocity formulation were also defined as the solver properties. The Volume of fluid (VOF) method was set as the multiphase model with Geo-Reconstruct scheme. The material properties were defined by selecting from the FLUENT data base before the phase properties were specified. The primary and secondary phases were water and toluene, respectively. The surface tension between water and toluene was set at 0.0371 N/m (Dessimoz et al., 2008). Then the boundary conditions were specified. Constant velocities which are normal to the boundary were specified for the velocity inlet type boundaries. No-slip condition was used on the wall of the microchannel and guideline structures. For the unmodified surface simulation case,

37° of an averaged bare glass contact angle of water in toluene (Aota et al., 2009) was applied on the whole surface of the model. In the modified surface case, the bare glass contact angle was applied only on the water part and the silanized surface contact angle was applied on the wall of organic part.

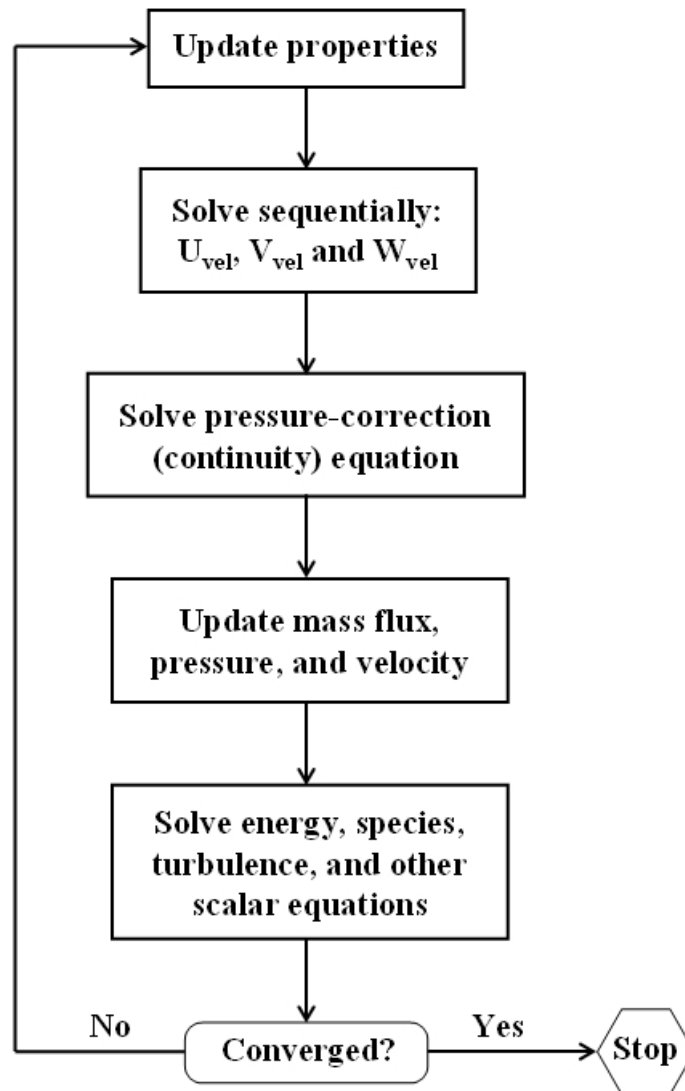


Figure 4.11 Pressure-based segregated algorithm (ANSYS Inc., 2009)

The silanized surface contact angle was determined by an experiment. A clean Pyrex glass capillary with 0.37 mm inside diameter surface was modified using octadecyltrichlorosilane (OTS) as a silane agent. After rinsing with ethanol, the capillary was pretreated by 1M NaOH for 30 min. Then it was rinsed with distilled water and dried at 110°C for 1 h. The capillary was also pretreated with HCl 1M for 1 h before rinsing with distilled water, ethanol and acetone, respectively. After drying at 110°C for 1 h, it was immersed in a freshly prepared 15% OTS by volume solution in toluene for 20 h. The capillary was rinsed again with toluene and acetone and finally dried at 110°C for 1 h. Then the contact angles were measured from the images. The silanized capillary was wet with water and filled with dyed toluene and water to make an interface wall contact. The angles were observed and the photos were taken through a microscope. Figure 4.12 shows the contact angle images before silanization (θ_1) and after silanization (θ_2). The three times averaged silanized contact angle of 143° was specified at the organic part wall in the modified surface simulation case.

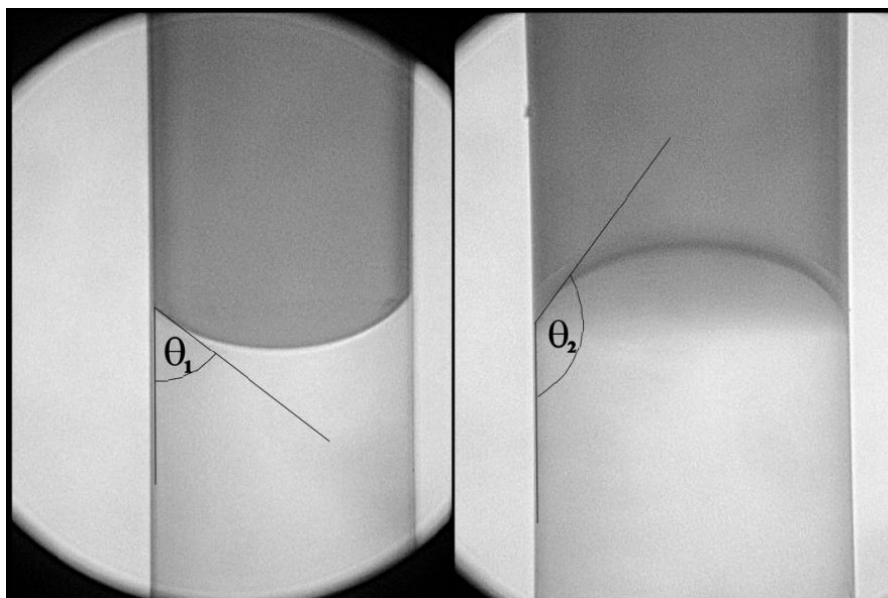


Figure 4.12 Contact angles of water (clear phase) in toluene (dyed phase) on the glass surface before (left) and after (right) silanization

e. Solve the Problem in FLUENT

The PISO pressure-velocity coupling, the PRESTO pressure discretisation scheme and the Second Order Upwind momentum discretisation scheme were defined as the solution controls. The channel was initialized with water. The convergence criteria were set. The time step size, the number of time steps and the maximum iterations per time step were specified before iterating solution.

f. Analyze the results

The simulation results were compared to examine the effect of guideline structure and surface modification on the stable flow pattern and flow development behavior. Also, the feed flow rate and ratio effects were analyzed to find the appropriate conditions for the parallel flow and the separation performance. Finally, the size of microchannel was investigated. The results were displayed as the phase volume fraction contour and velocity vectors.

4.2.2 3D curved microchannel

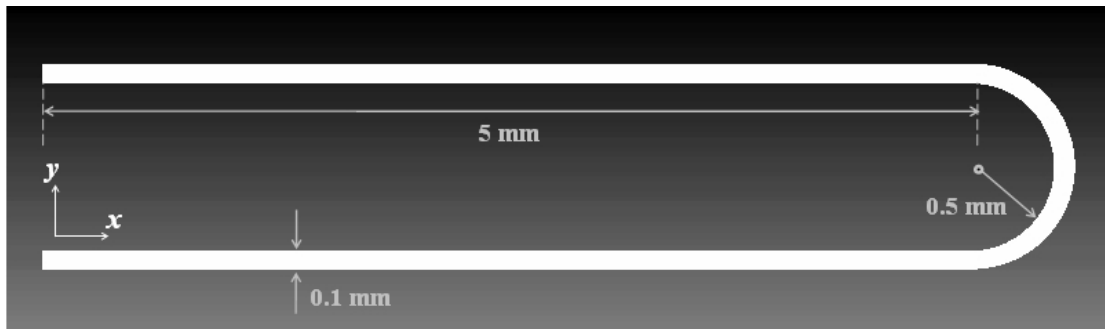
a. Create geometry in GAMBIT

The 3D model of curved microchannel as shown in Figure 4.13 was generated in GAMBIT. The channel dimension was based on the standard type product of Institute of Microchemical Technology Co.,Ltd. (IMT).

The same dimension microchannel model with guideline was also created to study the effect on the flow characteristic. The guideline wall and interval lengths were 100 μm as the same as model A in straight microchannel case.

The effect of the bend on the parallel flow pattern was studied by varying the curvature radius. The microchannels with curve radius of 1 and 3 mm were also created.

(a)



(b)

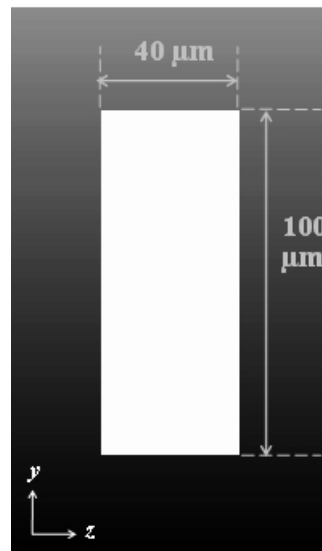
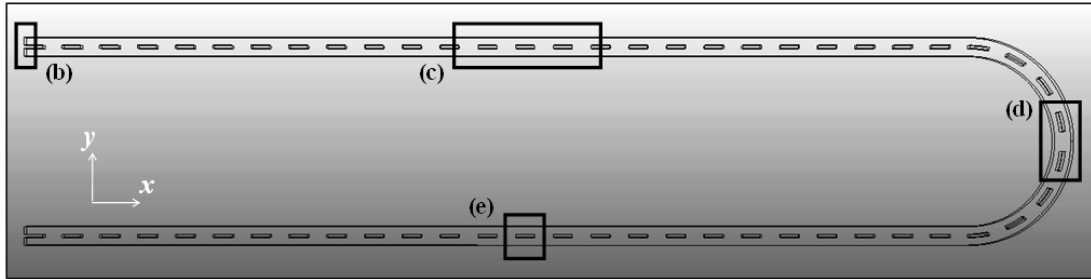


Figure 4.13 Curved microchannel with 0.5 mm curvature radius (a) top view and (b) cross section view

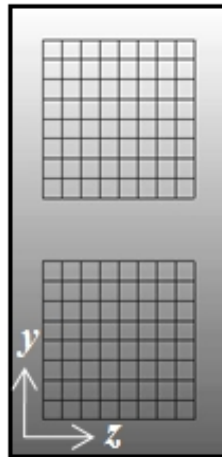
b. Mesh geometry in GAMBIT

The created microchannel models were mesh in GAMBIT. Without guideline structure, the 0.5, 1 and 3 mm curvature radius microchannels have 50,000, 60,000 and 90,000 cells, respectively. For the guided microchannel case, the model has 51,776 cells. Figure 4.14 shows the model outline and meshed model parts of microchannel with guideline structure. The meshed parts in Figure 4.14 (b)-(e) were enlarged from the rectangle areas in the outline in Figure 4.14 (a). In Figure 4.14 (e), the black lines are wall grids and white lines are interior grids.

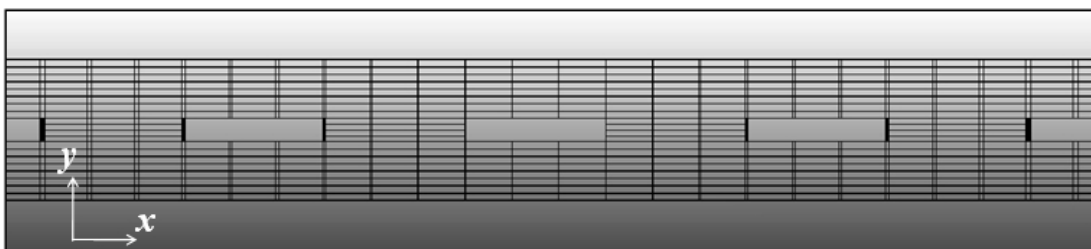
(a)



(b)



(c)



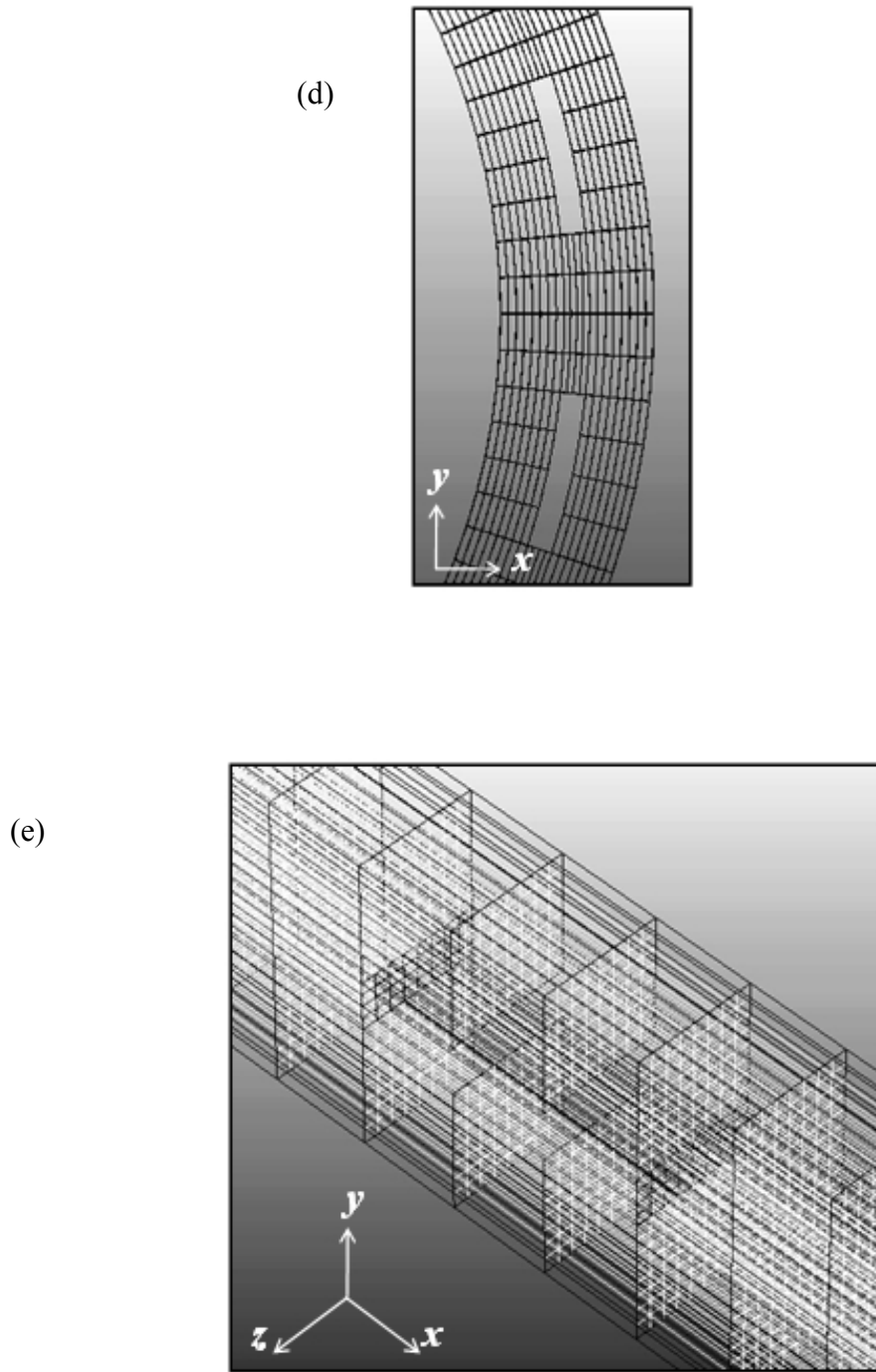


Figure 4.14 Meshed microchannel with guideline structure (a) outline, (b) inlet, (c) wall, (d) curve and (e) wall with interior meshes

c. Specify boundary types in GAMBIT

In GAMBIT, the boundary types were also specified. The water and toluene were fed in parallel to generate the layered flow. Because the curved channel is not symmetry, two inlet arrangements for outer and inner sides of the channel curve were created. Both inlets were defined as the velocity inlet in both cases. The water and toluene outlets, which were corresponded to the inlet arrangement, were set as outflow. The rest faces were specified as wall type.

The effect of surface modification was also investigated in the curved channel. The surface was divided into two parts in the modified surface case as mention before in the straight microchannel part.

The meshes were saved and exported to FLUENT.

d. Set up the problem in FLUENT

As in 2D, the 3D meshes were imported to FLUENT before checking error and scaling. The pressure-based solver, transient flow and absolute velocity formulation were also defined as the solver properties. The Volume of fluid (VOF) method was set as the multiphase model. Primary and secondary phases were water and toluene. Then the boundary conditions were specified. Constant velocities which are normal to the boundary were specified for the velocity inlet type boundaries. No-slip condition was used on the wall of the microchannel and guideline. The contact angles were specified at modified and unmodified wall surfaces.

e. Solve the problem in FLUENT

The PISO scheme was set for the pressure-velocity coupling. The PRESTO, the Second Order Upwind and the Geo-reconstruct were defined as pressure, momentum and volume fraction discretisation scheme, respectively. First order implicit was defined as the transient formulation. The channel was initialized with water. The convergence criteria were set. The time step size, the number of time steps and the maximum iterations per time step were specified before iterating solution.

f. Analyze the results

The simulation results were compared to examine the effect of guideline structure and surface modification on the parallel flow pattern. Also, the effect of curvature radius was studied. The results were displayed as the phase volume fraction contour and velocity vectors. In 3D simulation, both top view and cross section view results were analyzed. Figure 4.15 shows the cross section plane position specified in FLUENT.

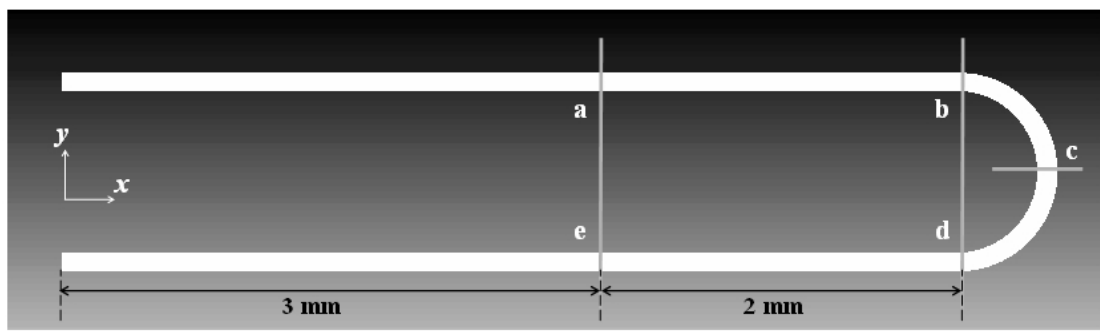


Figure 4.15 Cross section plane position

CHAPTER V

RESULTS AND DISCUSSION

The effect of guideline structure and surface modification on the organic-aqueous stable flow pattern and flow development behavior before stabilizing will be discussed in both straight and curved microchannel using CFD method. The commercial software, Fluent 6.3 and 12.0, was used to simulate in 2D and 3D. Toluene and water were used as organic and aqueous phases, respectively. All simulation cases were simulated until the flow patterns did not change with time. All simulation results are colored by phase. For color graphics, blue color represent water and red is toluene. For gray scale graphics, dark and light gray are water and toluene, respectively.

5.1 Effect of guideline structure in straight microchannel

In order to stabilize the two phase parallel flow pattern, adding the guideline structure into the middle of straight microchannel was proposed. The simulation flow pattern was compared with the published experimental result. Different guideline structures were considered to study the effect on the flow pattern. The role of guideline on the fluid behavior was also discussed.

With 10^{-7} time step size, when the feed flow rates of water and toluene were set equal at 0.01 ml/min, the simulation phase volume fraction contour of model A, which based on the TSR13 model in the experimental work (Tagawa et al., 2007), shows the stable parallel flow. The simulation flow pattern at 0.0148 s is shown in Figure 5.1 (a) which is in good agreement with that observed from the experiment in Figure 5.1 (b). This serpentine flow induced by guideline wall in liquid-liquid system was also reported by Maruyama et al. (2004).

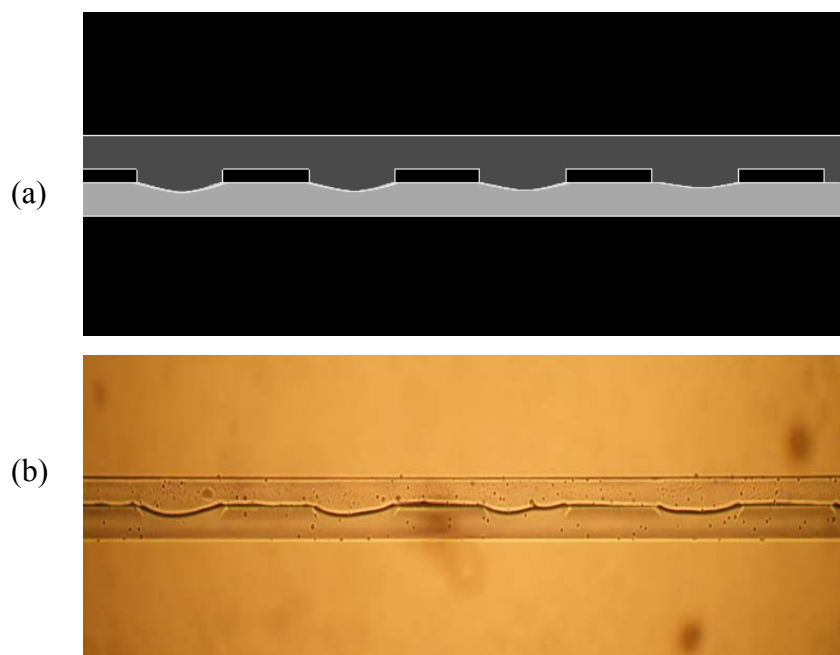


Figure 5.1 (a) Simulated stable parallel flow pattern of model A at 0.0148 s and
(b) experimental observation

The simulated flow development at the same each phase feed flow rates of 0.01 ml/min from feeding to stabilizing in the microchannel model A, B and C are shown in Figure 5.2, 5.3 and 5.4, respectively. In model A, the forefront part of the organic phase was spread in the entire channel and was guided to form two layered parallel flow by the guideline. The parallel flow was gradually stabilized with time. The spread toluene part in model B which possesses a larger interval was longer than model A. While the interface of model A was stable after 0.0124 s, model B seems to need more time to be stabilized. These results show that the guideline can help the fluid keep in their corresponding parts. The interface near the exits of model A was much more flat and stable than model B. Therefore, model A may provide better phase separation than model B. In contrast, the interface in model C was more unstable. Although the interface of model C was near the center along the length of microreactor, the interface position was changed with time in entire simulation time. This instability makes the separation uncontrollable.

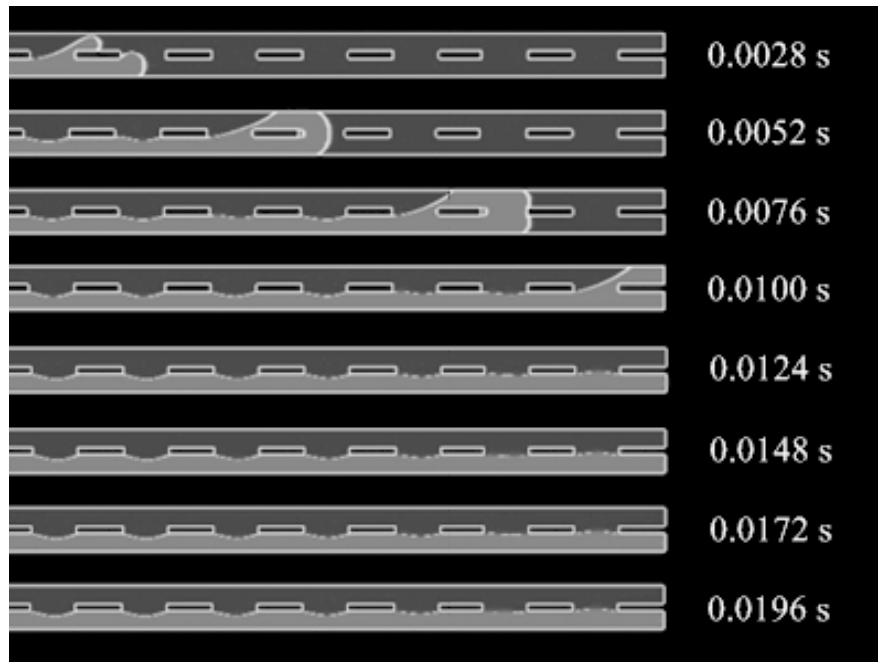


Figure 5.2 Flow development in model A

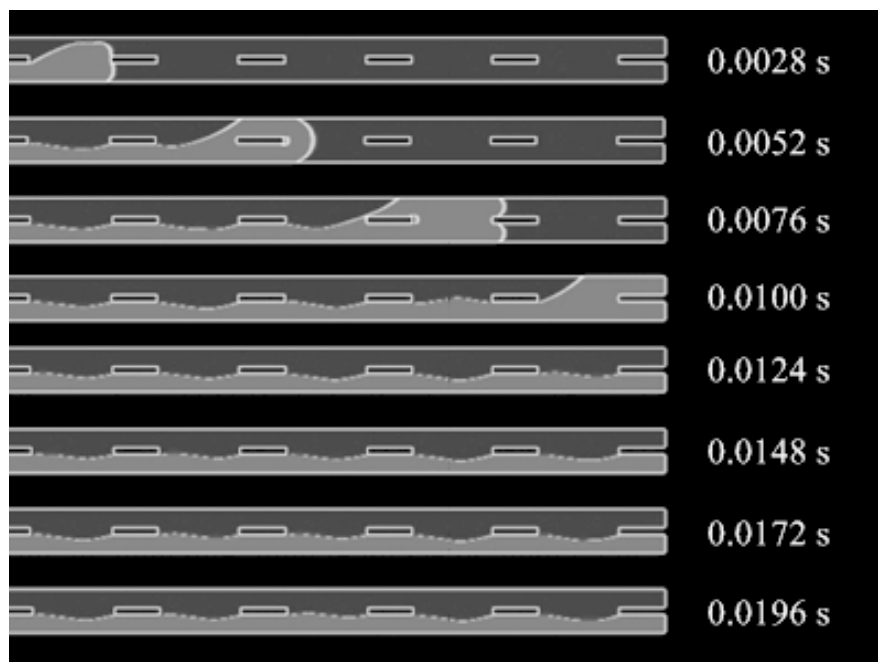


Figure 5.3 Flow development in model B

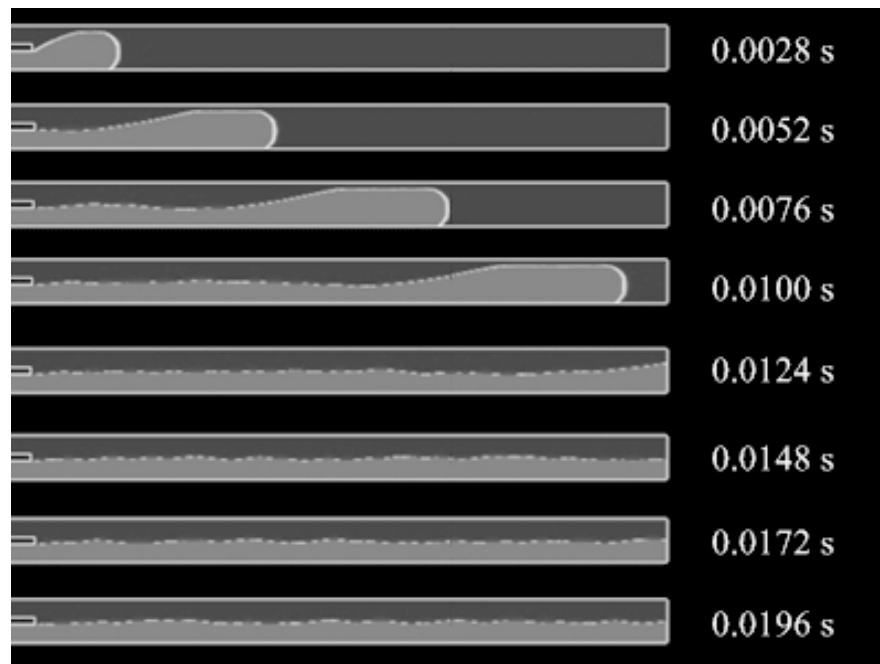


Figure 5.4 Flow development in model C

As reported by Tagawa et al. (2007), the flow instability was observed with decreasing flow rate. The simulation results of lower flow rates in model A are shown in Figure 5.5. The waving of the interface shown in Figure 5.5 (a) was found at each phase feed flow rate of 0.0025 ml/min. With further decreasing the flow rate, as the same as typical two phase flow in microchannel, the flow pattern was finally changed from the parallel flow to the slug flow at 0.0005 ml/min as in Figure 5.5 (b).

Figure 5.6 shows the effect of guideline on the parallel flow development in microchannel. At each phase flow rate of 0.01 ml/min, when the toluene stream reached each guideline structure, it was divided into two parts. After passing the wall, the interface was pushed toward the corner of the wall and broken. Then the fluids were guided in their own lanes.

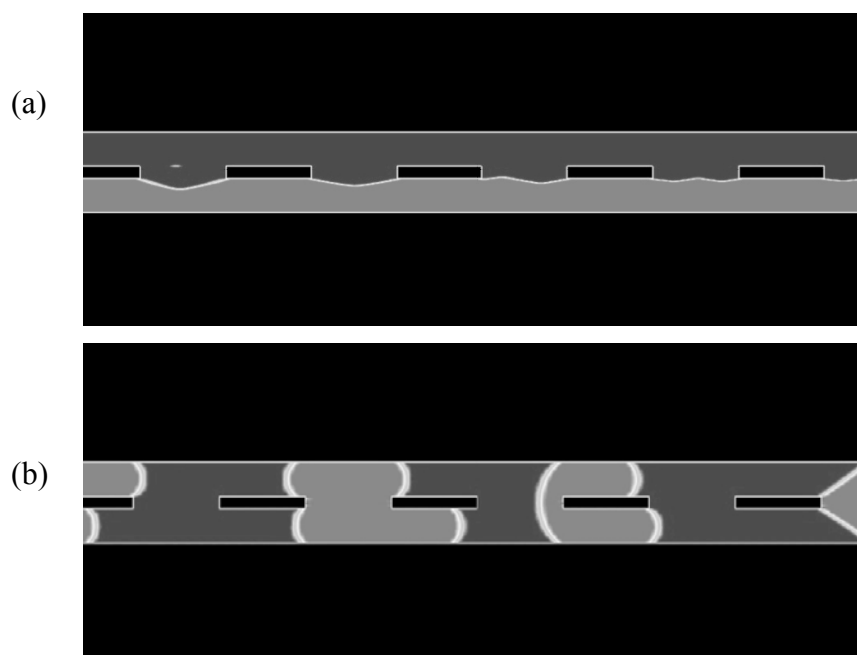


Figure 5.5 Simulated flow pattern of model A at (a) 0.0025 ml/min, (b) 0.0005 ml/min

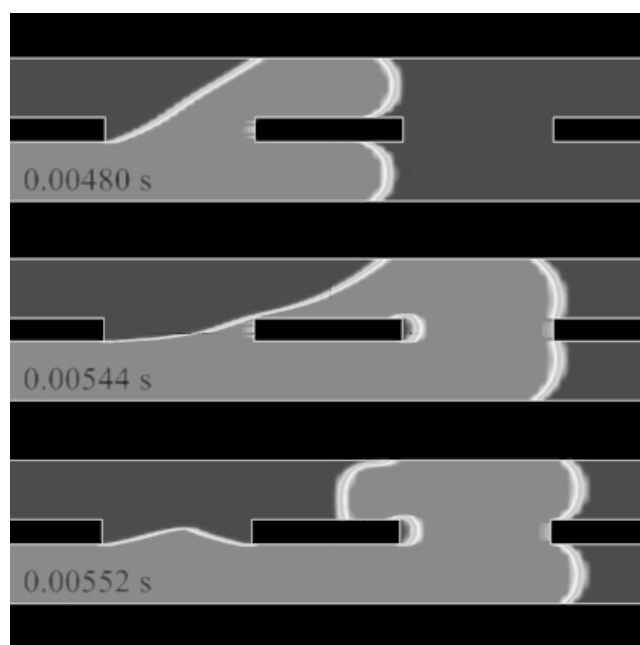
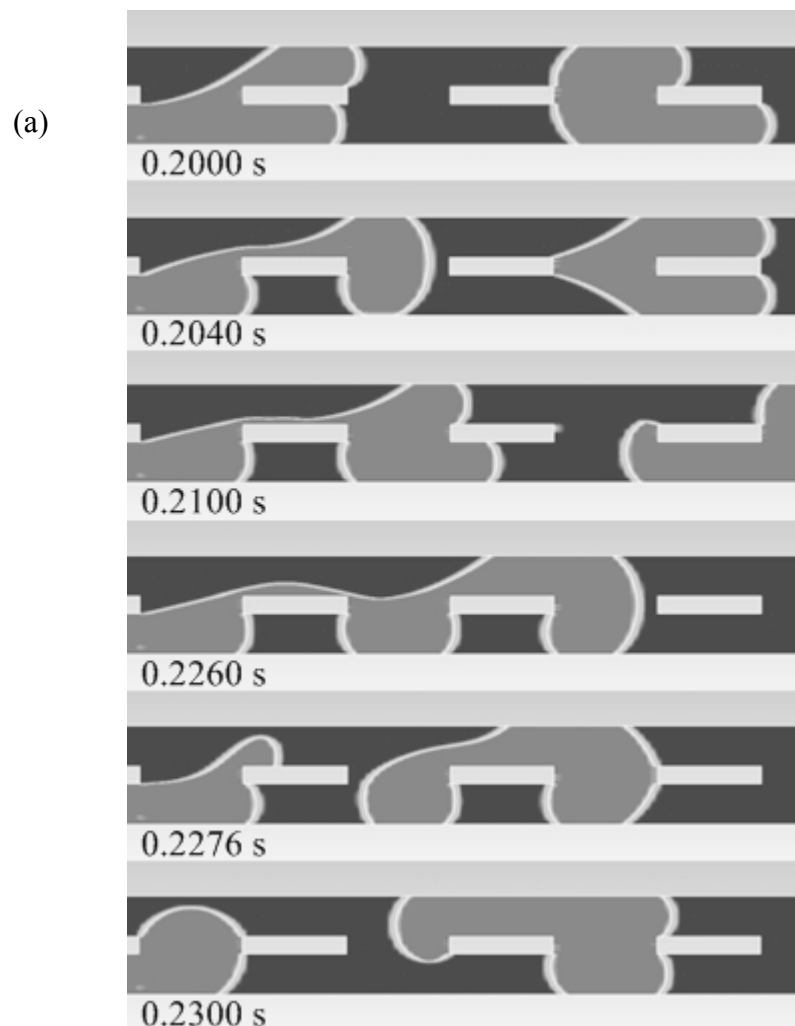


Figure 5.6 Movement of the forefront part of toluene in model A passing each guideline structure in parallel flow pattern

The role of guideline wall was also investigated in slug flow pattern at 0.0005 ml/min. As can be seen in Figure 5.7 (a), while the forefront of the toluene stream was passing the first guideline structure, the upper part was faster and spread over the channel width at the interval. The toluene under the wall moved back and amount of water was locked between the toluene under that wall. The toluene stream was broken by the front edge (or by the back edge as shown in Figure 5.7 (b)) of the wall. Therefore, water became surround that broken toluene part. The slugs were random flowed above and below guideline structures along the channel.



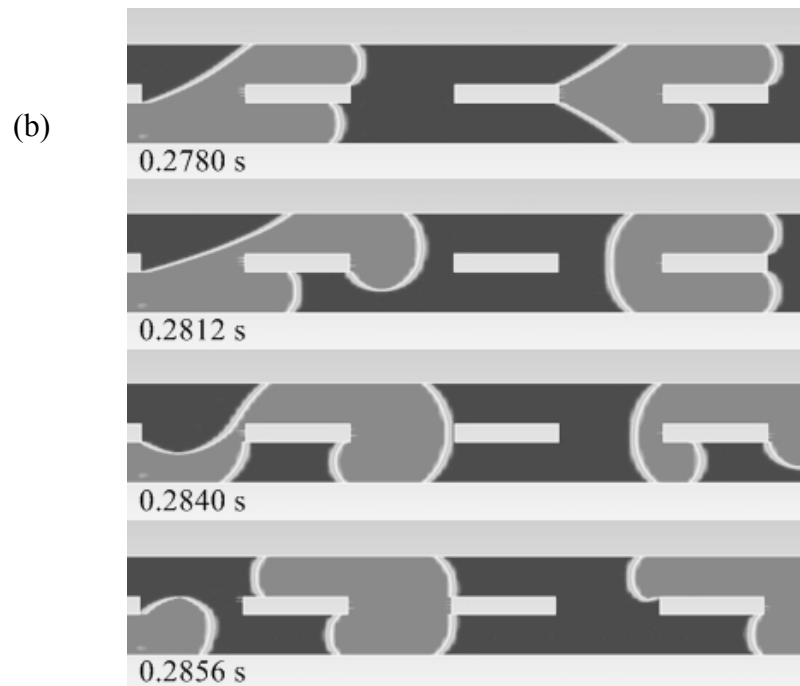


Figure 5.7 Movement of the forefront part of toluene in model A passing each guideline structure at near inlet in slug flow pattern which broken at (a) the front edge and (b) the back edge

The simulation velocity vectors of parallel flow at each phase flow rate of 0.01 ml/min in the middle of the microchannel length of model A, B and C are displayed in the left of Figure 5.8 from top to bottom, respectively. The interface between the guideline walls in model A and B was shifted to the toluene phase, so the toluene velocity was faster than water that results in longer vector arrows. Because of the flow instability in model C, the flow velocity direction of the fluids near interface was varying with roughly equal magnitude. With guideline structure, the velocity vector directions in model A and B are almost parallel to the interfaces. However the aqueous phase flow nearby the interface collides with guideline walls and the small swirling flows, which may help mixing, were observed at the edge of the walls as shown in the right of the figure. The vortex pictures were enlarged from the yellow rectangles on the left.

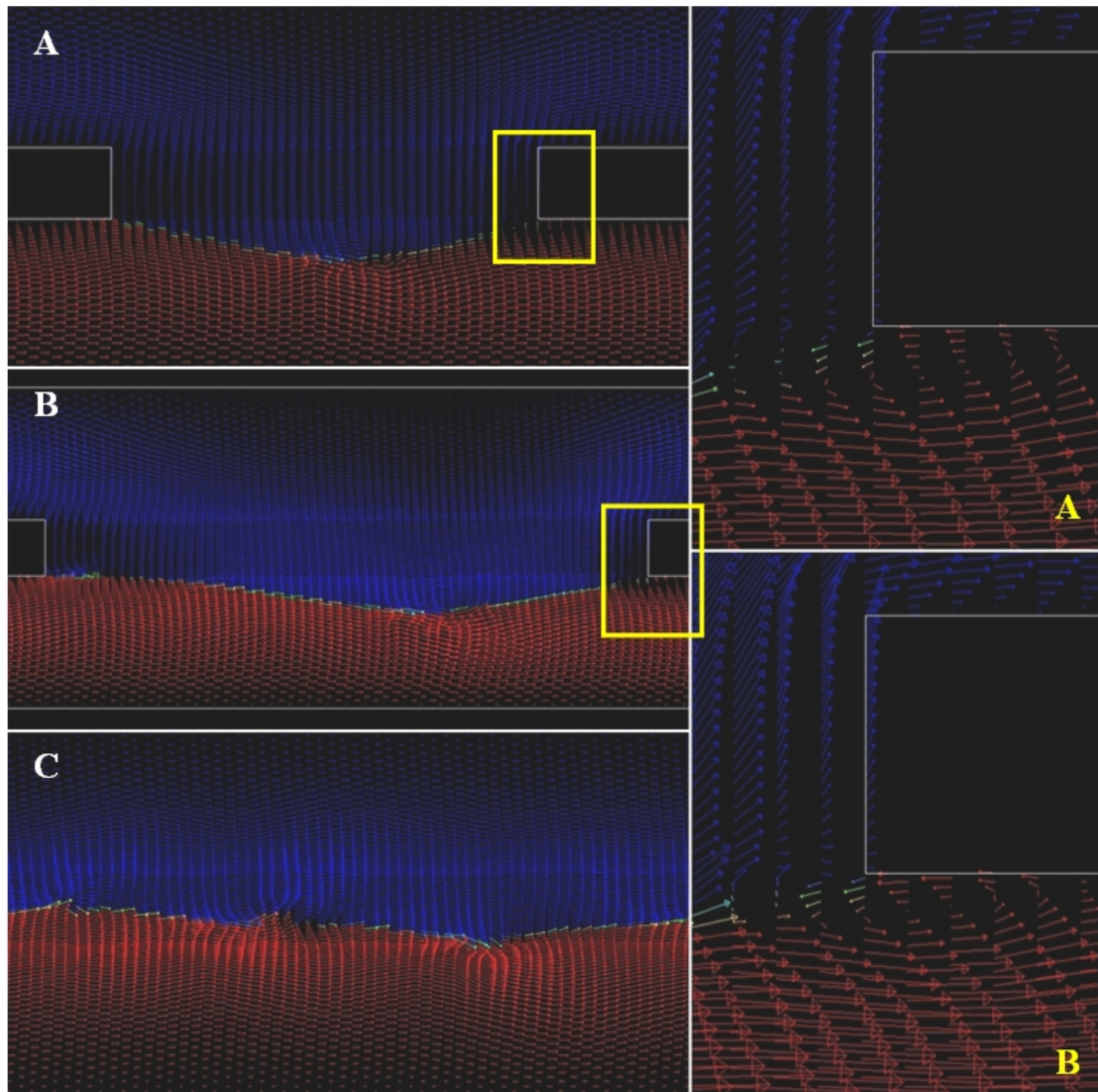


Figure 5.8 Velocity vectors at 0.01 ml/min in model A, B and C

For slug flow at each phase flow rate of 0.0005 ml/min, the velocity fields of a slug moving pass the guideline structure are shown in Figure 5.9. In contrast to the parallel flow, many swirling flows were observed near the guideline wall and interface.

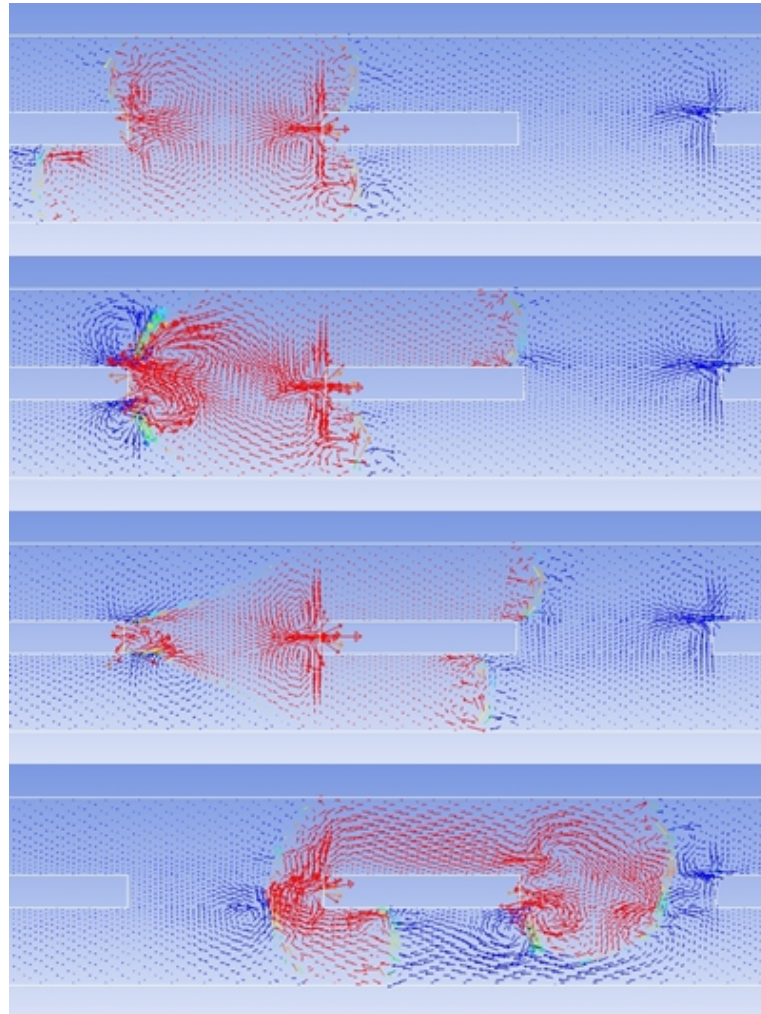


Figure 5.9 Velocity vectors at 0.0005 ml/min of a moving slug in model A

5.2 Effect of surface modification in straight microchannel

From the effect of guideline study, the parallel flow can be guided by the intermittent wall but the toluene phase still leak into the water part at the beginning. The other proposed method is surface modification by silanization. To improve the parallel flow, surface modification was introduced in the microchannel with guideline structure model A which provided the best result in the earlier study. The effect of surface modification on the flow pattern was analyzed by comparing with the unmodified microchannel case. The effect on flow pattern transition was also

investigated. In addition, the flow rate and ratio effects on the flow pattern were clarified. Finally, the effect of microchannel width was also investigated.

With the same feed flow rate of water and toluene at 0.01 ml/min, the simulation flow development in the microchannel without and with surface modification are shown in Figures 5.10 and 5.11, respectively. While the top part of the toluene feed in the bare glass microchannel spread into the water lane, both phases in the modified channel were maintained in their lanes since feeding. When the time to stabilize the interface was considered, it took more than 0.0100 s in the unmodified case but required less time in the modified surface microchannel.

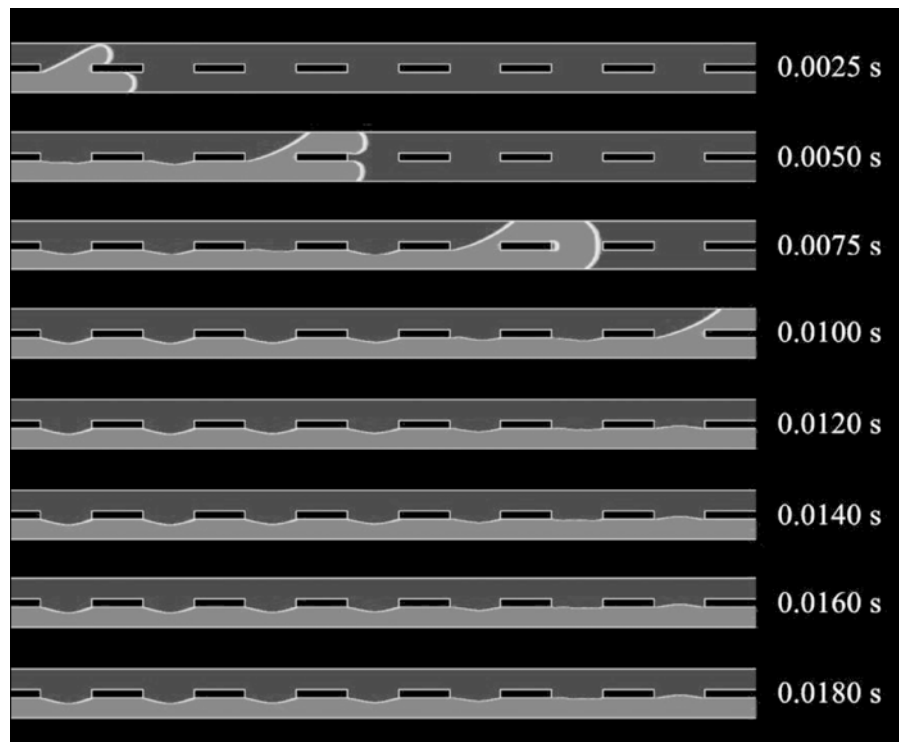


Figure 5.10 Flow development in the unmodified microchannel at the same phase feed flow rate at 0.01 ml/min

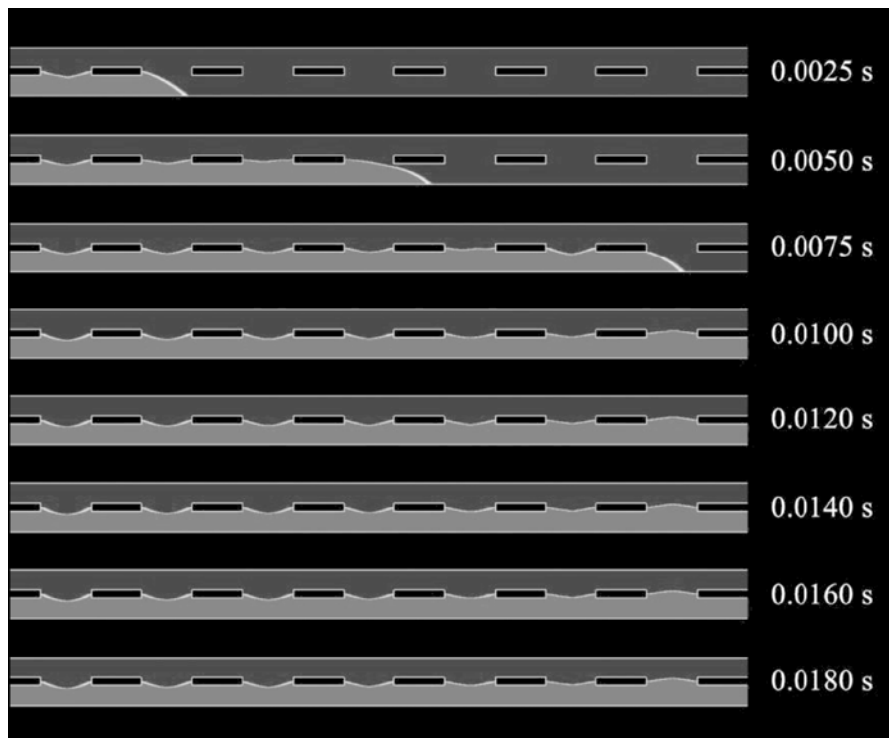


Figure 5.11 Flow development in the modified microchannel at the same phase feed flow rate at 0.01 ml/min

For the unmodified microchannel, the simulated flow pattern at 0.0140 s is enlarged in Figure 5.12 (a). The stabilized interface was curved between the guideline structures. When the simulation result was compared to the modified surface case shown in Figure 5.12 (b), the interface wall contact position is shifted from the edge of the guideline to the middle of the lateral side which is the separated point between modified and unmodified surfaces in the channel. Thus better separation can be expected in the surface modification case.

As report in previous topic, the flow pattern in the unmodified surface microchannel was changed from the parallel flow to the slug flow at 0.0005 ml/min. On the contrary, the simulated flow pattern at the same condition in the modified microchannel was parallel flow as shown in Figure 5.13. Therefore, the surface modification can alter the flow pattern transition in microchannel.

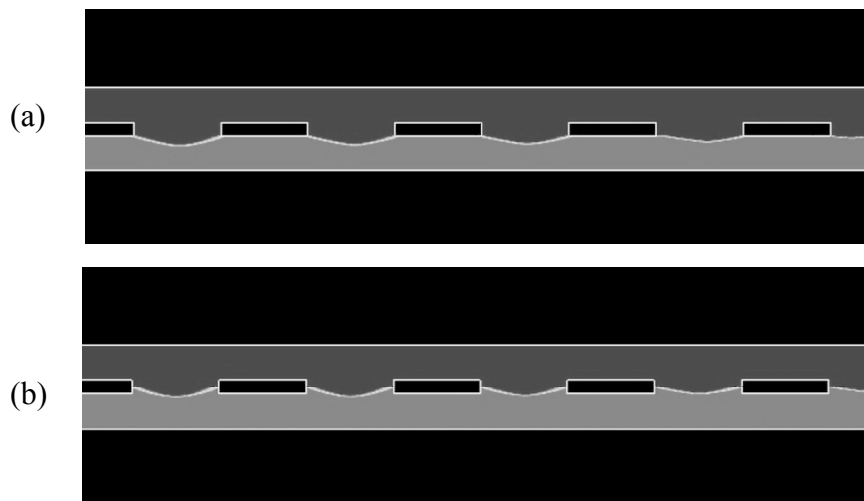


Figure 5.12 Simulated flow patterns at the same phase feed flow rate at 0.01 ml/min of (a) unmodified microchannel, (b) modified surface microchannel

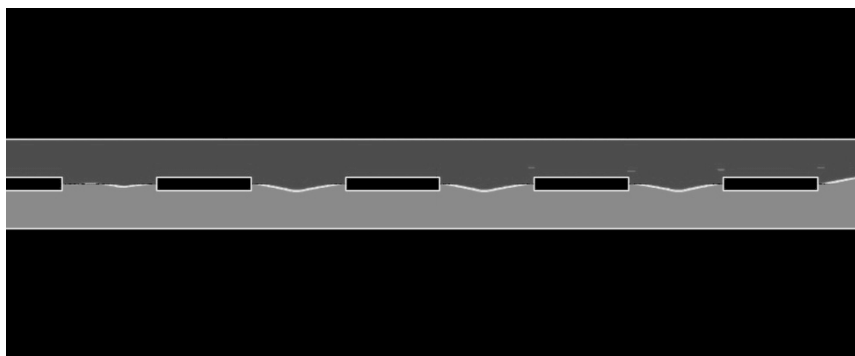


Figure 5.13 Simulated flow pattern of modified microchannel at 0.0005 ml/min

The feed flow rate was increased to enhance the throughput. Figure 5.14 and 5.15 show the flow patterns with different flow rates in the unmodified and modified surface microchannel, respectively. The interface shows instability with different behaviors between that two cases when the feed flow rate was further increased after stabilizing. From both case results, by increasing each phase feed flow rate to 0.015 ml/min, the interface shape became more curved. At 0.02 ml/min, the interface is shifted to the toluene lane and the guideline is totally surrounded by water in the unmodified channel. With higher flow rate, the interface was wavier. For the modified channel, at each feed flow rate of 0.02 ml/min, one of the contact points in each interval moves back from the middle of the channel to the edge of the guideline wall. When the flow rate was further increased, the fluids cannot be retained in their own paths and spread into the other lane. With increasing flow rate, there are more droplets and being smaller in size.

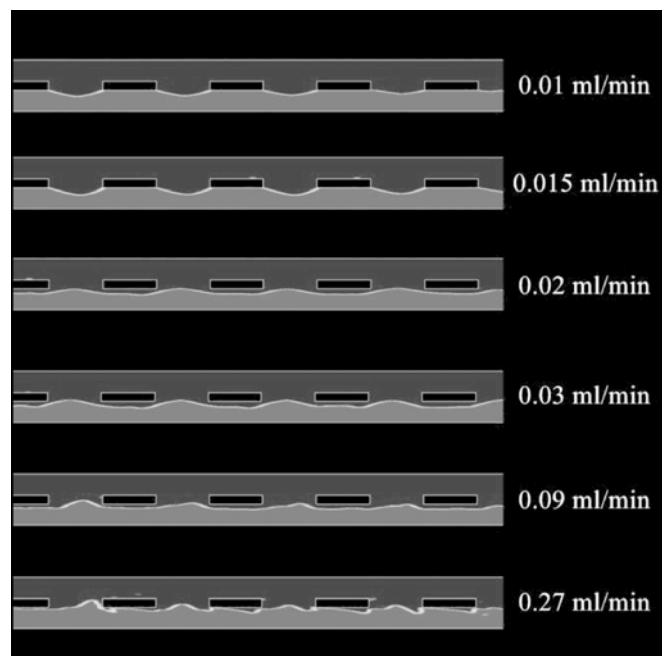


Figure 5.14 Simulated flow patterns of unmodified microchannel at different phase feed flow rates

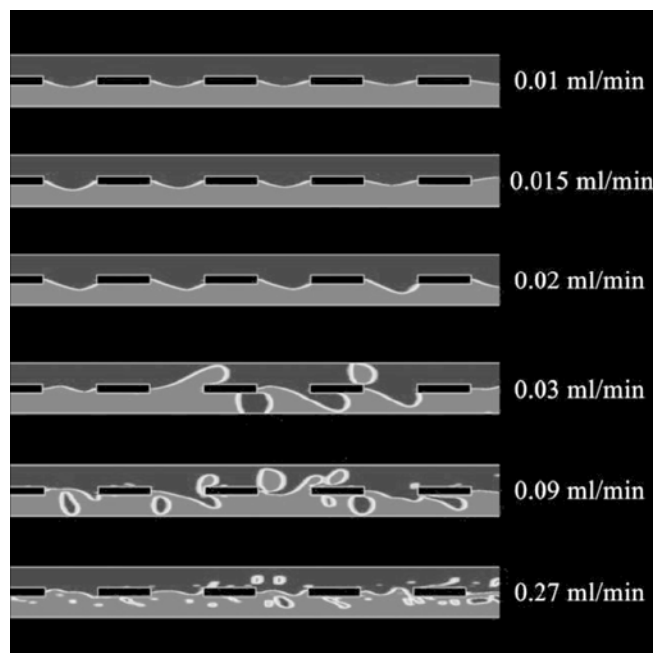


Figure 5.15 Simulated flow patterns of modified microchannel at different phase feed flow rates

Although the parallel flow patterns are unstable at higher flow rate, the interface and therefore, the phase separation performance can be improved by adjusting the feed flow rate ratio. As report by Aljbour et al. (2010), the leakage of the aqueous phase to the organic phase decreases with the increasing organic-to-aqueous flow rate ratio. Figure 5.16 and 5.17 show the simulated flow patterns with different toluene-to-water flow rate ratios at the constant toluene flow rates of 0.02 and 0.03 ml/min, respectively. When increasing the ratio, the interface could be stabilized and showed less curvature. At the fixed organic phase flow rate of 0.02 ml/min, one of the interface wall contact points was on the middle of the microchannel but the other one was on the edge of the partition wall at the same phase feed flow rate. However the contact points can be both attached at the channel center when the ratio was increased to 1.2. Furthermore, the scattered flow at equal phase feed flow rate of 0.03 ml/min could be changed to parallel flow by increasing the ratio to 1.3. The interface were started to be wavy when the ratio were further increased.

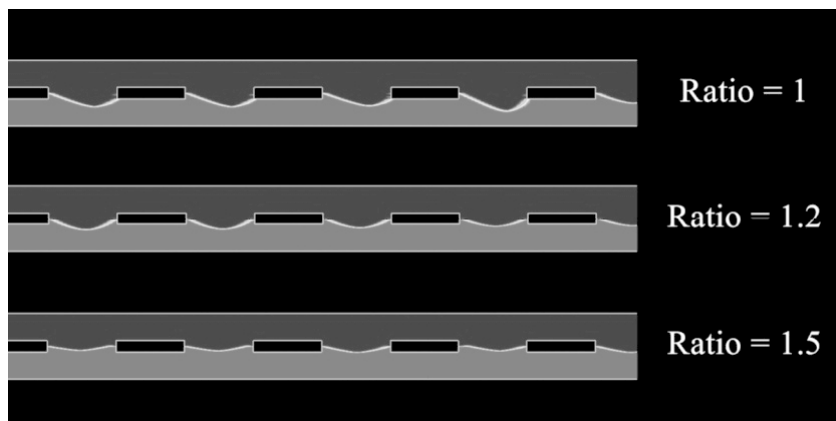


Figure 5.16 Simulated flow patterns of modified microchannel at different feed flow rate ratio with fixed organic phase flow rate of 0.02 ml/min

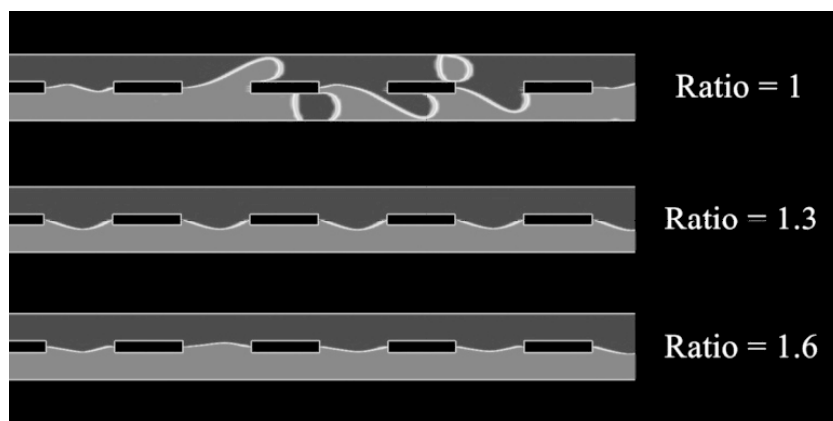


Figure 5.17 Simulated flow patterns of modified microchannel at different feed flow rate ratio with fixed organic phase flow rate of 0.03 ml/min

The effect of microchannel size was also investigated in both unmodified and modified surface cases. The microchannel with the same guideline structure models with double and half widths were generated and simulated at the same phase feed flow rates of 0.02 ml/min. For the double width case, the simulation results show that the interfaces shifted towards the aqueous phase in both with and without surface modification channels as shown in Figure 5.18 and 5.19. When the diameter is increased, the velocity is also decreased. With different viscosities, this cause the lower flow pressure difference between the phases, and therefore, the interface move to the aqueous phase which is the opposite direction to the increasing flow rate result. With the surface modification, the Laplace pressure is changed to a range and the phases will not leak when the flow pressure differences do not exceed that range.

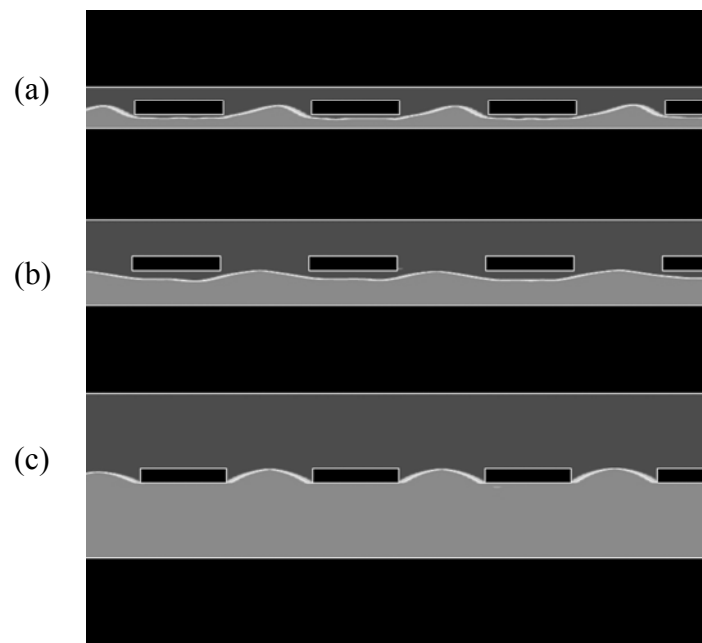


Figure 5.18 Simulated flow patterns of unmodified microchannel at the phase flow rate of 0.02 ml/min with (a) a half width, (b) a normal width and (c) a double width

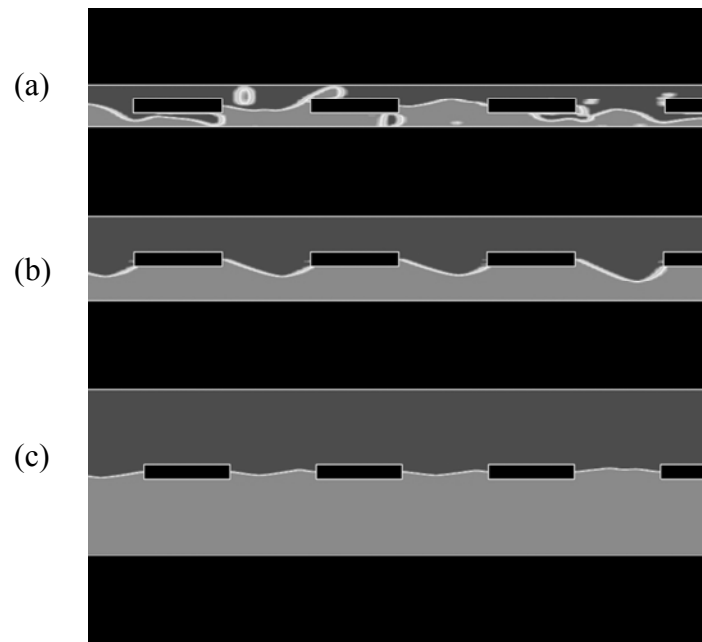


Figure 5.19 Simulated flow patterns of modified microchannel at the phase flow rate of 0.02 ml/min with (a) a half width, (b) a normal width and (c) a double width

5.3 Effect of guideline structure and surface modification in curved microchannel

Although the straight microchannels have been studied and applied in many works, the serpentine channel is widely used because of its compactness. Thus flow pattern and the effect of parallel flow stabilizing methods, adding guideline structure and modifying surface, were studied in the curved microchannel in this topic. The flow velocity vectors were also investigated.

With the same curvature radius at 0.5 mm, five feed flow rates, 0.025, 0.0625, 0.25, 0.5, 1 ml/min of each phase were simulated in plain, modified surface and guided microchannel. Two cases of inlet position were also considered, toluene in the outer lane with water in the inner lane and water in the outer lane with toluene in the inner lane of the curve.

In the curved microchannel without any modification, the simulated stable flow patterns in the straight part before curve were parallel flows which the interfaces were shifted to the toluene phases. By investigating the y - z plane cross section, the interface showed more curve and the toluene phase took less area at the higher flow rate. This is consistent with the 2D simulation result that the interface was shifted to the toluene phase when the flow rate was increased. Figure 5.20 shows the volume fraction contours of 0.025 and 1 ml/min phase feed flow rates with outer water lane at the position b cross section in Figure 4.14.

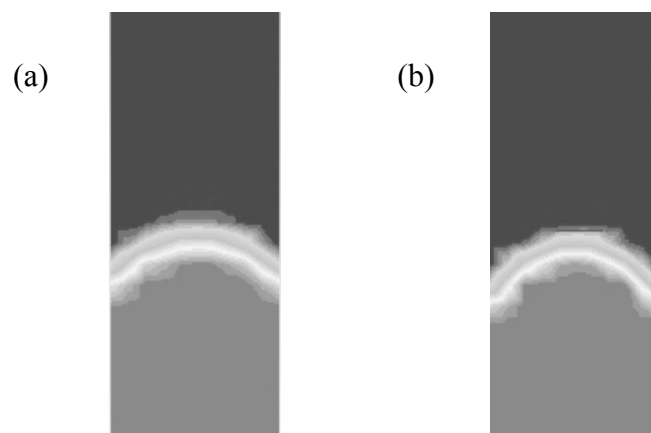


Figure 5.20 Volume fractions in curved microchannel without modification at position b of (a) 0.025 and (b) 1 ml/min with outer water lane

The flow patterns after passing the bend are shown in Table 5.1. When toluene was fed at the outer path, the flow patterns after turn were still parallel in all flow rates. But the flow patterns were changed to annular and phase switch parallel at the feed rates of 0.5 and 1 ml/min, respectively, in the case that water was in the outer lane. Figures 5.21 shows the different flow patterns observed in the microchannel without modification.

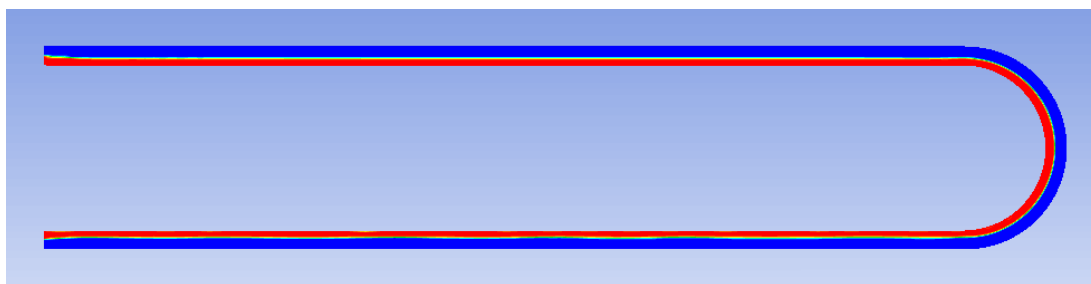
Table 5.1 Flow patterns after bend in microchannel without modification

Outer phase	Flow rate (ml/min)				
	0.025	0.0625	0.25	0.5	1
Toluene	Parallel	Parallel	Parallel	Parallel	Parallel
Water	Parallel	Parallel	Parallel	Annular	Phase switch

(a)



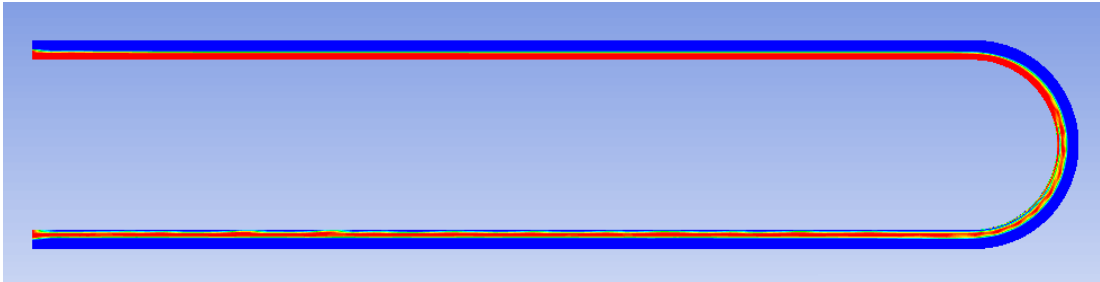
(b)



(c)



(d)



(e)

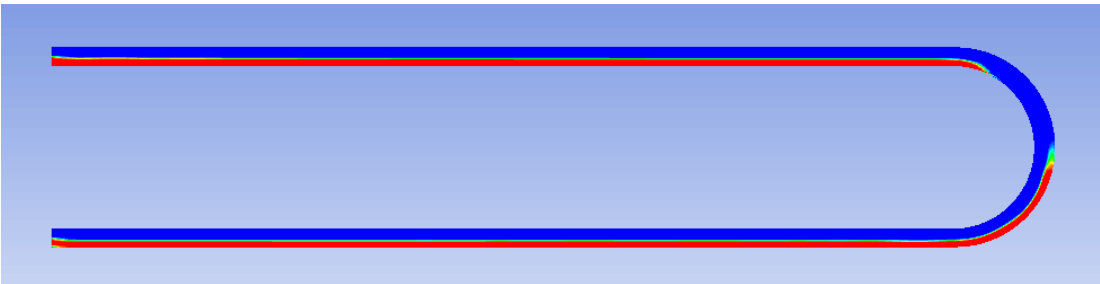



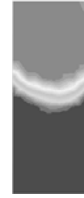
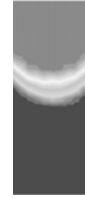
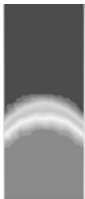
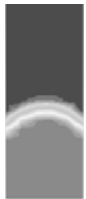

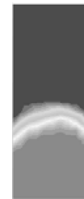
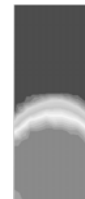



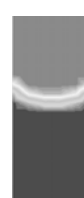









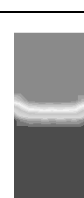



Figure 5.21 Flow patterns in plain cured microchannel of phase feed flow rates at (a) 0.025 ml/min with outer toluene, (b) 0.025 ml/min with outer water, (c) 0.5 ml/min min with outer toluene, (d) 0.5 ml/min min with outer water and (e) 1 ml/min with outer water

The cross section volume fraction contours of the parallel, annular and phase switch parallel patterns in Figures 5.21 at position a-e are shown in Table 5.2. The top side of all contours in the table is outer part of the microchannel. In parallel flow pattern, the interface shape did not change significantly between each position. The water gradually surrounded the toluene stream in the annular case. In the phase switch case, the toluene stream move from inner to outer lane after entering the curve part and was surrounded by water at the position c. After that the side water films were disappeared and the parallel flow with flat interface was observed at the position d. The flat interface was developed to the curved interface again as shown in position e.

Table 5.2 Volume fractions at position a-e of parallel, annular and phase switch flow patterns in curved microchannel without modification

Flow rate (ml/min), Outer phase	Flow pattern	Position				
		a	b	c	d	e
0.025, Toluene	Parallel					
0.025, Water	Parallel					
0.5, Toluene	Parallel					
0.5, Water	Annular					
1, Water	Phase switch					

The centrifugal instability of a fluid flow inside a curved tube can be explained by dimensionless Dean number. With constant channel diameter and curvature radius, the number is increased with the Reynolds number. Comparing between toluene and water, the Reynolds number of toluene is greater at the same velocity and channel diameter. Thus the centrifugal force, which acts towards the outer wall, in toluene is stronger than in water. This might cause the toluene stream dislocation when it was fed at the inner path of the curve at high flow rate.

From the results, the system with bend could not maintain the parallel flow when the flow rate was too high. In order to stabilize the parallel flow, guideline structure and surface modification method were applied in the curved microchannel.

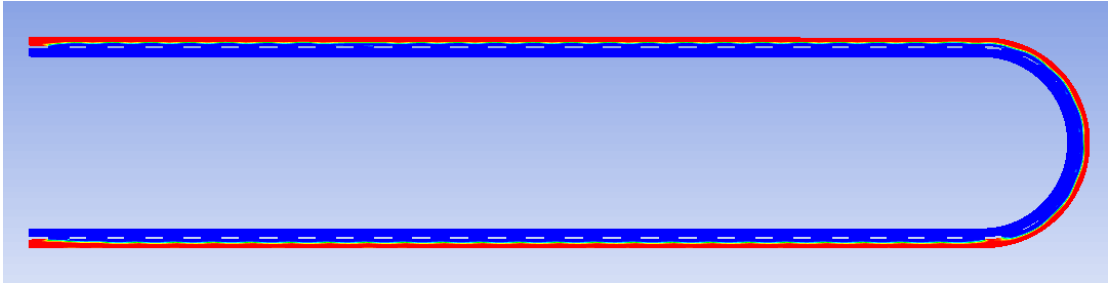
With guideline structure, the simulated stable flow patterns in the straight part before curve were parallel flows which the interfaces were shifted to the toluene path in all simulation flow rate range as the same as in plain curved microchannel. The flow patterns after passing the bend are shown in Table 5.3.

Table 5.3 Flow patterns after bend in microchannel with guideline structure

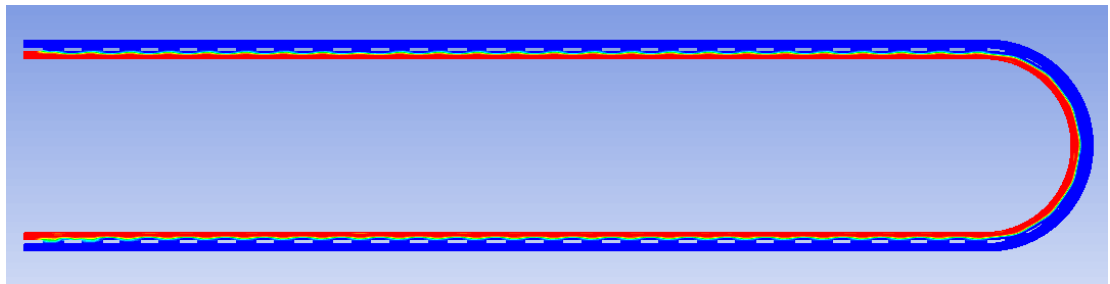
Outer phase	Flow rate (ml/min)				
	0.025	0.0625	0.25	0.5	1
Toluene	Parallel	Parallel	Parallel	Parallel	Parallel
Water	Parallel	Parallel	Parallel	Annular	Annular

As in microchannel without modification, when toluene was fed at the outer path, the flow patterns after turn were still parallel in all flow rates. But the flow patterns were changed to annular flows at the feed rates of 0.5 and 1 ml/min in the case that water was in the outer lane. Comparing to the plain microchannel, the guideline structure could not use to parallelize the flow pattern in this operation range. Figure 5.22 shows the parallel and annular flow in microchannel with guideline wall.

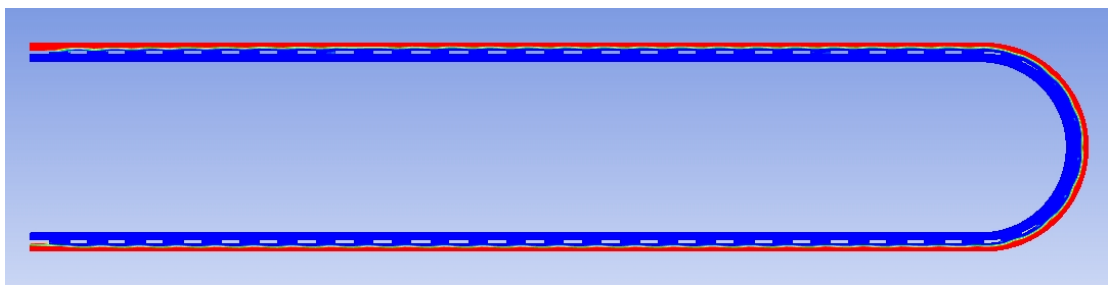
(a)



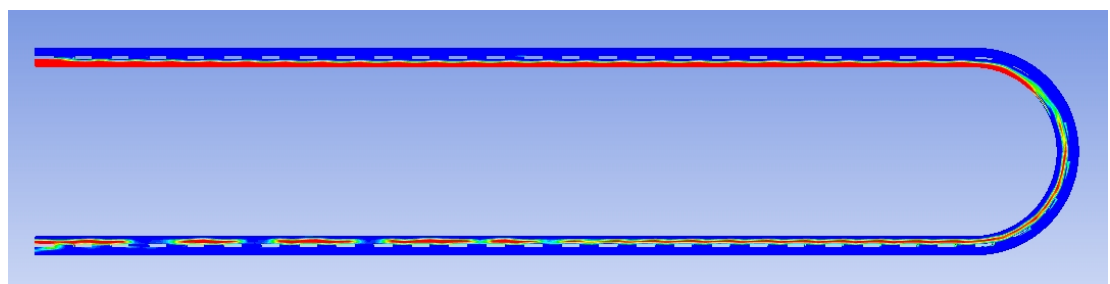
(b)



(c)



(d)



(e)

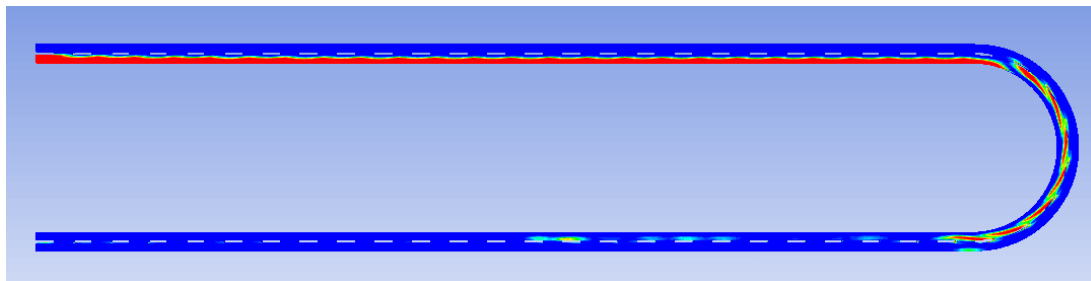





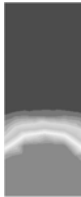
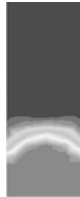











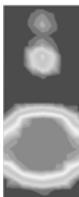
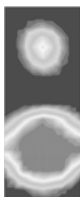







Figure 5.22 Flow patterns in cured microchannel with guideline structure of phase feed flow rates at (a) 0.025 ml/min with outer toluene, (b) 0.025 ml/min with outer water, (c) 0.5 ml/min min with outer toluene, (d) 0.5 ml/min min with outer water and (e) 1 ml/min with outer water

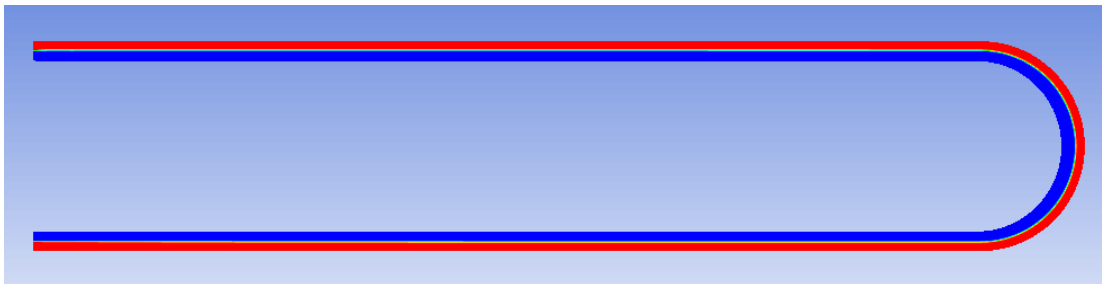
The cross section volume fraction contours of the parallel, annular and phase switch parallel patterns in Figures 5.22 at position a-e are shown in Table 5.4. The interface shapes were similar to the case without modification but there were smaller area of toluene phase at 0.025 ml/min and 0.05 ml/min with outer toluene. Therefore, the toluene streams were confined by the guideline wall. At higher flow rate, water became surround the toluene as in without modification case before dividing into two or more parts by the guideline wall. Thus the guideline structure could not improve the flow pattern and the phase separation in this system.

Table 5.4 Volume fractions at position a-e of parallel, annular and phase switch flow patterns in curved microchannel with guideline structure

Flow rate (ml/min), Outer phase	Flow pattern	Position				
		a	b	c	d	e
0.025, Toluene	Parallel					
0.025, Water	Parallel					
0.5, Toluene	Parallel					
0.5, Water	Annular					
1, Water	Annular					

When the surface modification method was applied, all flow patterns both before and after turn in the simulation range were parallel as shown in Figure 5.23. For all flow rates, the interfaces observed in x-y plane were posed at the middle of the microchannel width.

(a)



(b)

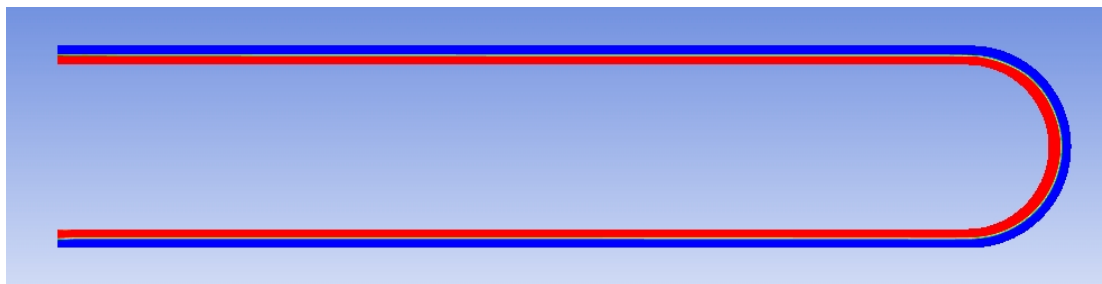



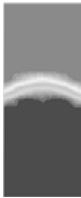
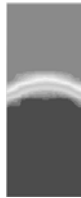
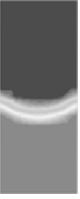



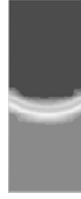





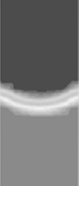


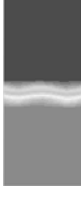



Figure 5.23 Flow patterns in cured microchannel with surface modification of phase feed flow rates at (a) 0.025 ml/min with outer toluene and (b) 1 ml/min with outer water

Although there was no difference observed from the top view, the interfaces in the cross section view showed the unlike behaviors. The cross section volume fraction contours at flow rates of 1 and 0.025 ml/h at a-e positions are shown in Table 5.5. As can be seen, at low flow rate, the curved interfaces were not changed along the channel both water and toluene outer phases. But it was perturbed by the bend at high flow rate. However, the interface return to the shape as in position a at position e. The

velocity was the largest near the middle of the channel and therefore, the centrifugal force was the strongest at there.

Table 5.5 Volume fractions at position a-e cross section of parallel flow patterns in curved microchannel with surface modification

Flow rate (ml/min), Outer phase	Position				
	a	b	c	d	e
0.025, Toluene					
0.025, Water					
1, Toluene					
1, Water					

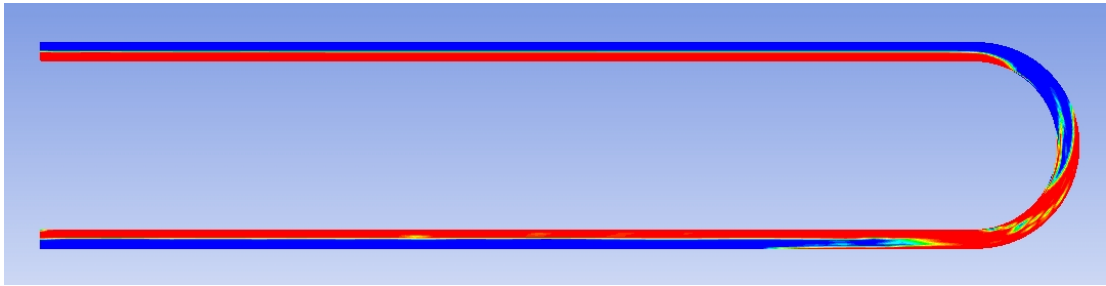
When the velocity field was considered, only the results at 0.025 ml/min show the non-uniform velocity vector directions in all cases. The velocity vectors and their side views of flow rates of 0.025 and 1 ml/min in microchannel without modification at positions a, c and e are shown in Table 5.6. Considering based on the Capillary number, the ratio of viscous force over the interfacial forces is decreased when the flow rate is minimized. The instability at lower flow rate is caused by the interfacial forces, which act on the interface, dominated. The pattern of velocity vectors at position c were changed in both flow rates by the influence of the curvature. At 0.025 ml/min, there were two vortices observed similar to the single phase dean vortices. For 1 ml/min, the velocity direction and the maximum velocity magnitude were shifted to the outer phase. These velocity vector changes may help improving transport processes.

However, in microchannel with modified surface, when the flow rate was further increased from 1 ml/min, the system could not maintain the parallel flow pattern as shown in Figure 5.24. The flow patterns at 1 ml/min in plain microchannel were also investigated with curvature radius of 1 and 3 mm. The contour at 1 mm radius shows the phase switch at the curve similar to that in channel with 0.5 mm radius. However, the result in 3 mm curve radius channel shows the annular pattern as shown in Figure 5.25 which is similar to the result at flow rate of 0.5 ml/min in channel with 0.5 mm radius. From the results, the stable parallel flow pattern was expected at larger curve radius.

Table 5.6 Velocity vectors at position a, c and e cross section in curved microchannel without modification

Flow rate (ml/min), Outer phase	Position					
	a		c		e	
0.025, Toluene						
0.025, Water						
1, Toluene						
1, Water						

(a)



(b)

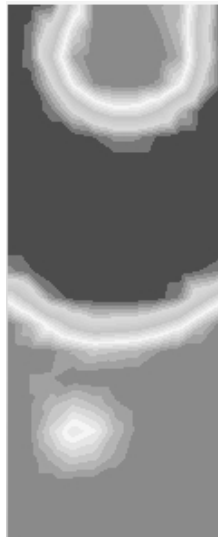
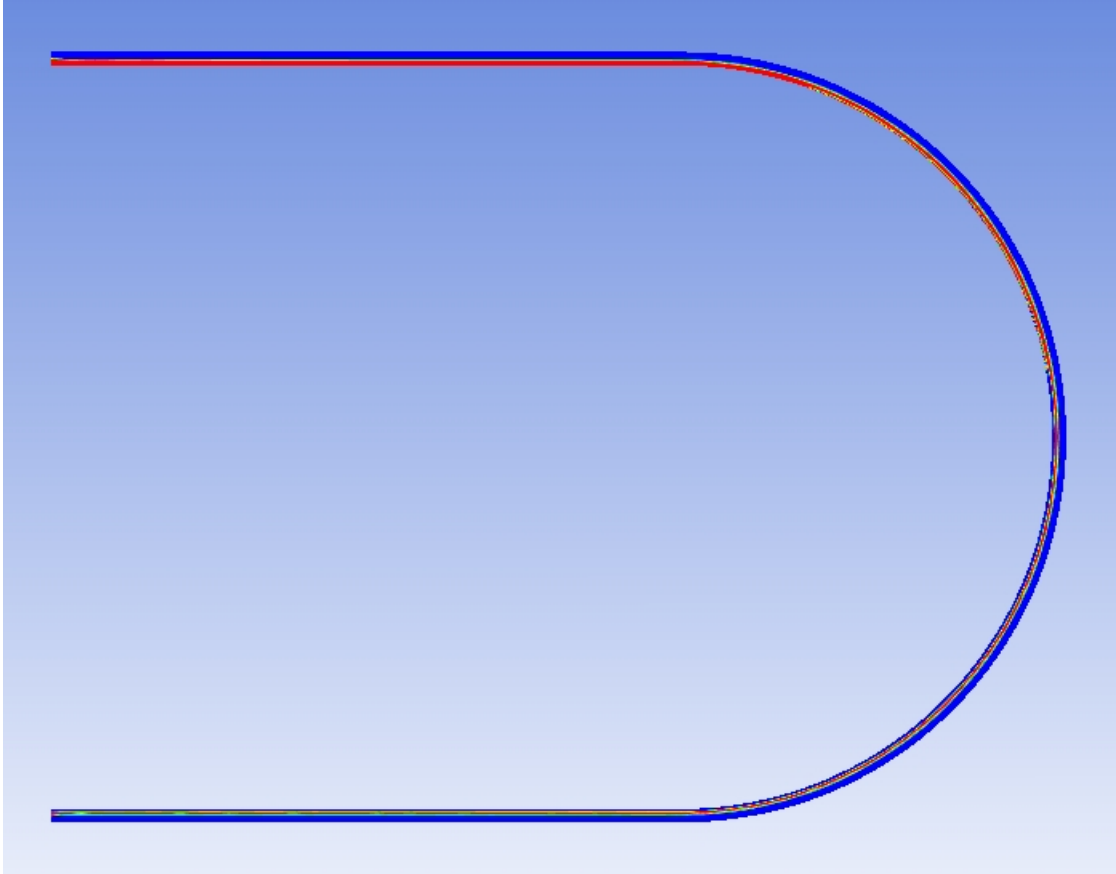


Figure 5.24 Flow pattern at 3 ml/min in microchannel with surface modification in (a) top view and (b) cross section at position e

(a)



(b)

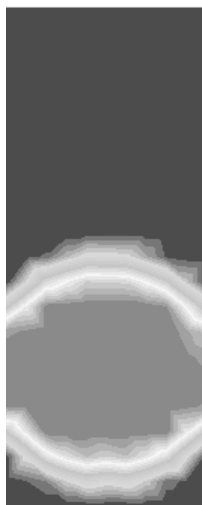


Figure 5.25 Flow pattern at 1 ml/min in plain microchannel with 3 mm curvature radius in (a) top view and (b) cross section at position e

CHAPTER VI

CONCLUSIONS AND RECOMMENDATIONS

The flow behaviors and parallel flow stabilization methods were studied in this research by applying CFD method. The results from the investigation are summarized. The recommendations of future work are also suggested.

6.1 Conclusions

6.1.1 Guideline structure

The serpentine and stable flow was induced by the intermittent guideline wall. This simulated flow shape was agreed with the experimental results. However the wall could not help stabilizing the parallel flow both in straight and curved microchannels in the inappropriate flow rate range.

6.1.2 Surface modification

The surface modification clearly helps shifting the interface wall contact point to the center of the microchannel. In the case that flow pattern was stabilized by guideline structure, surface modification further improved the flow development to maintain the fluids in their own path. With high flow rate, which the interface was posed in the toluene channel and could not be stabilized by the structure, the interface position could be adjusted by varying the flow rate ratio. At low flow rate, which the flow transition to slug occurs, the surface modification can maintain the parallel flow pattern.

In the curved microchannel, at high flow rate that the inner toluene stream detached from their corresponding path, the surface modification can also maintain

the parallel flow pattern. Moreover, the perturbed interface at the curve could completely return to the observed shape before the bend.

6.1.3 CFD method

The top and bottom walls were not considered in 2D simulation. As can be seen in 3D simulation, the actual cross section interface shows curve shape as the effect of surface wettability. Therefore, the 2D and 3D results should be similar if the contact angle of the system is around 90° . In this work, because the interface is curved, the complete phase separation by two outlets may be difficult to be obtained. However, one phase in its outlet with a trace of the other phase can be expected. From the results, 2D simulation could predict the effects of geometries, surface properties and flow conditions while, 3D simulation could well provide more accurate results and the flow detail information. Thus, the criteria for choosing 2D and 3D are the model geometric symmetry, the level of accuracy and the required information.

Therefore, by using CFD, the appropriate design, which provides the desired flow pattern, can be fundamentally estimated.

6.2 Recommendations

There are two types of guideline structure, intermittent and continuous. The intermittent wall was studied in this research. It is interesting to study the effect of continuous wall and compare the interface stabilization, the contact area and the velocity vector results with the intermittent type. So the appropriate guideline type can be selected.

By silanization, the clean surface is covered by silinol cross-linked film. There are many pretreatment procedures have been used in literatures. The effect of pretreatment method on the contact angle, film unity and stability should be further considered.

To design the microchannel for a specific application, the parameters such as the inlet, outlet and channel geometries and dimensions, the curvature radius, the

reactor material and the parallel improvement technique should be varied thoroughly in the CFD study.

Due to the computer resource, the grid resolution and time step size were limited in this research. For more accurate results, the simulation should be done in higher performance computational machine.

REFERENCES

- Akbar, M.K., Plummer, D.A. and Ghiaasiaan, S.M. On gas-liquid two-phase flow regimes in microchannels. International Journal of Multiphase Flow 29 (2003): 855–865.
- Aljbour, S., Tagawa, T., Matouq, M. and Yamada, H. Multiphase surfactant-assisted reaction-separation system in a microchannel reactor. Frontiers of Chemical Engineering in China 3 (1 SPEC. ISS.), (2009a): 33–38.
- Aljbour, S., Yamada, H. and Tagawa, T. Rate enhanced and green ethoxylation of p-Chloronitrobenzene in a microchannel reactor. Journal of Chemical Engineering of Japan 42 (SUPPL. 1), (2008): 90–95.
- Aljbour, S., Yamada, H. and Tagawa, T. Sequential Reaction-Separation in a Microchannel Reactor for Liquid–Liquid Phase Transfer Catalysis. Topics in Catalysis 53 (2010): 694–699.
- Aljbour, S., Yamada, H. and Tagawa, T. Simultaneous reaction-separation in a microchannel reactor with the aid of a guideline structure. International Journal of Chemical and Biomolecular Engineering 2 (2009b): 220–223.
- Al-Yaari, M., Soleimani, A., Abu-Sharkh, B., Al-Mubaiyedh, U. and Al-sarkhi, A. Effect of drag reducing polymers on oil-water flow in a horizontal pipe. International Journal of Multiphase Flow 35 (2009): 516–524.
- Angeli, P. and Hewitt, G.F. Flow structure in horizontal oil-water flow. International Journal of Multiphase Flow 26 (2000): 1117–1140.
- ANSYS, Inc. ANSYS FLUENT 12.0 Theory Guide. USA: ANSYS, Inc., 2009.

- Aota, A., Hibara, A., and Kitamori, T. Pressure Balance at the Liquid-Liquid Interface of Micro Countercurrent Flows in Microchips Analytical Chemistry 79 (2007): 3919–3924.
- Aota, A., Mawatari, K., Takahashi, S., Matsumoto, T., Kanda, K., Anraku, R., Hibara, A., Tokeshi, M. and Kitamori, T. Phase separation of gas–liquid and liquid–liquid microflows in microchips. Microchim Acta 164 (2009): 249–255
- Atencia, J. and Beebe, D.J. Controlled microfluidic interfaces. Nature 437 (2005): 648–655.
- Balachandran, S. Verification of volume-of-fluid (VOF) simulation for thin liquid film applications. Proceedings of ICEE 2009 3rd International Conference on Energy and Environment 2009.
- Baroud, C.N. and Willaime, H. Multiphase flows in microfluidics. Comptes Rendus Physique 5 (2004): 547–555.
- Beretta, A., Ferrari, P., Galbiati, L. and Andreini, P.A. Horizontal oil-water flow in small diameter tubes. flow patterns. International Communications in Heat and Mass Transfer 24 (1997): 223–229.
- Brackbill, J.U., Kothe, D.B. and Zemach, C. A continuum method for modeling surface tension. Journal of Computational Physics 100 (1992): 335–354.
- Brauner, N. On the relations between two-phase flow under reduced gravity and earth experiment. International Communications in Heat and Mass Transfer 17 (1990): 271–281.
- Brennen, C.E. Fundamentals of Multiphase Flow. Cambridge University Press, 2005.
- Brzoska, J. B., Ben Azouz, I. and Rondelez, F. Silanization of Solid Substrates: A Step toward Reproducibility. Langmuir 10 (1994): 4367–4373.

- Burns, J.R. and Ramshaw, C. The intensification of rapid reactions in multiphase systems using slug flow in capillaries. Lab on a Chip 1 (2001): 10–15.
- Burns, J.R. and Ramshaw, C. A microreactor for the nitration of benzene and toluene. Chemical Engineering Communications 189 (2002): 1611–1628.
- Carson, G.A. and Granick, S. Self-assembly of octadecyltrichlorosilane monolayers on mica. Journal of Materials Research 5 (1990): 1745–1751.
- Chai, J., Lu, F., Li, B. and Kwok, D.Y. Wettability Interpretation of Oxygen Plasma Modified Poly(methyl methacrylate) Langmuir 20 (2004): 10919–10927
- Chen, I.Y., Chen, Y.M., Yang, B. and Wang, C. Two-phase flow pattern and frictional performance across small rectangular channels. Applied Thermal Engineering 29 (2009): 1309–1318.
- Dessimoz, A., Cavin, L., Renkena, A. and Kiwi-Minsker, L. Liquid-liquid two phase flow patterns and mass transfer characteristics in rectangular glass microreactors. Chemical Engineering Science 63 (2008): 4035–4044.
- Dreyfus, R., Tabeling, P., and Willaime H. Ordered and disordered patterns in two-phase flows in microchannels. Physical Review Letters 90 (2003): 144505/1–144505/4.
- Dummann, G., Quittmann, U., Gröschel, L., Agar, D.W., Wörz, O. and Morgenschweis, K. The capillary-microreactor: a new reactor concept for the intensification of heat and mass transfer in liquid-liquid reactions. Catalysis Today 79–80 (2003): 433–439.
- Ehrfeld, W., Hessel, V. and Löwe, H., Microreactors: New technology for modern chemistry. Germany: Wiley–VCH, 2000.
- Flinn, D.H., Guzonas, D.A. and Yoon R.-H. Characterization of silica surfaces hydrophobized by octadecyltrichlorosilane. Colloids and Surfaces A: Physicochemical and Engineering Aspects 87 (1994): 163–176.

Fluent Inc. FLUENT 6.3 User Guide. Lebanon: Fluent Inc., 2006

Fries, D.M. and Rudolf von Rohr, P. Impact of inlet design on mass transfer in gas–liquid rectangular microchannels. Microfluid Nanofluid 6 (2009b): 27–35

Fries, D.M. and Rudolf von Rohr, P. Liquid mixing in gas–liquid two-phase flow by meandering microchannels. Chemical Engineering Science 64 (2009a): 1326–1335

Fries, D.M., Waelchli, S. and Rudolf von Rohr, P. Gas–liquid two-phase flow in meandering microchannels Chemical Engineering Journal 135S (2008): S37–S45.

Glatzel, T., Litterst, C., Cupelli, C., Lindemann, T., Moosmann, C., Niekrawietz, R., Streule, W., Zengerle, R. and Koltay, P. Computational fluid dynamics (CFD) software tools for microfluidic applications - A case study. Computers & Fluids 37 (2008): 218–235.

Günther, A. and Jensen, K.F. Multiphase microfluidics: from flow characteristics to chemical and materials synthesis. Lab on a Chip 6 (2006): 1487–1503.

Guo, F. and Chen, Bin. Numerical Study on Taylor Bubble Formation in a Micro-channel T-Junction Using VOF Method Microgravity Science and Technology 21 (2009) (Suppl 1):S51–S58.

Harries, N., Burns, J.R., Barrow, D.A. and Ramshaw, C. A numerical model for segmented flow in a microreactor. International Journal of Heat and Mass Transfer 46 (2003): 3313–3322.

Hessel, V., Löwe, H., Müller, A. and Kolb, G. Chemical Micro Process Engineering. Germany: Wiley-VCH, 2005.

Hibara, A., Iwayama, S., Matsuoka, S., Ueno, M., Kikutani, Y., Tokeshi, M. and Kitamori, T. Surface Modification Method of Microchannels for Gas-Liquid Two-Phase Flow in Microchips Analytical Chemistry 77 (2005): 943–947.

- Hibara, A., Nonaka, M., Hisamoto, H., Uchiyama, K., Kikutani, Y., Tokeshi, M. and Kitamori, T. Stabilization of liquid interface and control of two-phase confluence and separation in glass microchips by utilizing octadecylsilane modification of microchannels. Analytical Chemistry 74 (2002): 1724–1728.
- Hibara, A., Tokeshi, M., Uchiyama, K., Hisamoto, H. and Kitamori, T. Integrated multilayer flow system on a microchip. Analytical Sciences 17 (2001): 89–93.
- Hirt, C.W. and Nichols, B.D. Volume of fluid (VOF) method for the dynamics of free boundaries. Journal of Computation Physics 39 (1982): 201–225.
- Hisamoto, H., Shimizu, Y., Uchiyama, K., Tokeshi, M., Kikutani, Y., Hibara, A. and Kitamori, T. Chemicofunctional Membrane for Integrated Chemical Processes on a Microchip Analytical Chemistry 75 (2003): 350–354.
- Huh, D., Kuo, C.-H., Grotberg, J.B. and Takayama, S. Gas–liquid two-phase flow patterns in rectangular polymeric microchannels: effect of surface wetting properties New Journal of Physics 11 (2009): 075034.
- Kashid, M.N. and Kiwi-Minsker, L. Microstructured Reactors for Multiphase Reactions: State of the Art Industrial and Engineering Chemistry Research 48 (2009): 6465–6485.
- Kashid, M.N., Agar, D.W. and Turek, S. CFD modelling of mass transfer with and without chemical reaction in the liquid-liquid slug flow microreactor. Chemical Engineering Science 62 (2007b): 5102–5109.
- Kashid, M.N., Fernández Rivas, D., Agar D. W. and Turek, S. On the hydrodynamics of liquid-liquid slug flow capillary microreactors. Asia-Pacific Journal of Chemical Engineering 3 (2008): 151–160.
- Kashid, M.N., Gerlach, I., Goetz, S., Franzke, J., Acker, J.F., Platte, F., Agar, D.W. and Turek, S. Internal Circulation within the Liquid Slugs of a Liquid-Liquid

- Slug-Flow Capillary Microreactor. Industrial and Engineering Chemistry Research 44 (2005): 5003–5010.
- Kashid, M.N., Renken, A. and Kiwi-Minsker, L. Influence of Flow Regime on Mass Transfer in Different Types of Microchannels Industrial and Engineering Chemistry Research 50 (2011): 6906–6914.
- Kockmann, N. Micro Process Engineering. Germany: Wiley-VCH, 2006.
- Kralj, J.G., Sahoo, H.R. and Jensen, K.F. Integrated continuous microfluidic liquid-liquid extraction. Lab on a Chip 7 (2007): 256–263.
- Kreutzer, M.T., Kapteijn, F., Moulijn, J.A. and Heiszwolf, J.J. Multiphase monolith reactors: Chemical reaction engineering of segmented flow in microchannels. Chemical Engineering Science 60 (2005): 5895–5916.
- Kulkarni, A.A. and Kalyani, V.S. Two-Phase Flow in Minichannels: Hydrodynamics, Pressure Drop, and Residence Time Distribution. Industrial and Engineering Chemistry Research 48 (2009): 8193–8204.
- Kumar, V., Vashisth, S., Hoarau, Y., Nigam, K.D.P. Slug flow in curved microreactors: Hydrodynamic study. Chemical Engineering Science 62 (2007) 7494–7504.
- Lin, R. and Tavlarides, L.L. Flow patterns of n-hexadecane-CO₂ liquid-liquid two-phase flow in vertical pipes under high pressure. International Journal of Multiphase Flow 35 (2009): 566–579.
- Liu, D. and Wang, S. Hydrodynamics of Taylor flow in noncircular capillaries. Chemical Engineering and Processing 47 (2008): 2098–2106.
- Lowe, D.C. and Rezkallah, K.S. Flow regime identification in microgravity two-phase flows using void fraction signals. International Journal of Multiphase Flow 25 (1999): 433–457.

- Lowe, H. and Ehrfeld, W. State-of-the-art in microreaction technology: concepts, manufacturing and applications. Electrochimica Acta 44 (1999): 3679–3689.
- Maruyama, T., Kaji, T., Ohkawa, T., Sotowa, K., Matsushita, H., Kubota, F., Kamiya, N., Kusakabe, K. and Goto, M. Intermittent partition walls promote solvent extraction of metal ions in a microfluidic device. The Analyst 129 (2004): 1008–1013.
- Maruyama, T., Uchida, J., Ohkawa, T., Futami, T., Katayama, K., Nishizawa, K., Sotowa, K., Kubota, F., Kamiya, N. and Goto, M. Enzymatic degradation of p-chlorophenol in a two-phase flow microchannel system. Lab on a Chip 3 (2003): 308–312.
- Meier, M., Yadigaroglu, G. and Smith, B.L. A novel technique for including surface tension in PLIC-VOF methods. European Journal of Mechanics B/Fluids 21 (2002): 61–73.
- Qian, D. and Lawal, A. Numerical study on gas and liquid slugs for Taylor flow in a T-junction microchannel. Chemical Engineering Science 61 (2006): 7609–7625.
- Reddy Cherlo, S.K., Kariveti, S. and Pushpavanam S. Experimental and Numerical Investigations of Two-Phase (Liquid-Liquid) Flow Behavior in Rectangular Microchannels. Industrial and Engineering Chemistry Research 49 (2010): 893–899.
- Reddy, V. and Zahn, J.D. Interfacial stabilization of organic–aqueous two-phase microflows for a miniaturized DNA extraction module. Journal of Colloid and Interface Science 286 (2005): 158–165.
- Reichen, P., Sonnenfeld, A. and Rudolf von Rohr, P. Remote plasma device for surface modification at atmospheric pressure plasma process. Plasma Processes and Polymers 6 (2009): S382–S386.

- Rezkallah, K.S. and Zhao, L. A flow pattern map for two-phase liquid-gas flows under reduced gravity conditions. Advances in Space Research 16 (1995): 133–136.
- Rezkallah, K.S. Weber number based flow-pattern maps for liquid-gas flows at microgravity. International Journal of Multiphase Flow 22 (1996): 1265–1270.
- Rosu, M. and Schumpe, A. Oxidation of glucose in suspensions of moderately hydrophobized palladium catalysts Chemical Engineering Science 65 (2010): 220–225.
- Salim, A., Fourar, M., Pironon, J. and Sausse, J. Oil–Water Two-Phase Flow in Microchannels: Flow Patterns and Pressure Drop Measurements. The Canadian Journal of Chemical Engineering 86 (2008): 978–988.
- Sinton, D. Microscale flow visualization. Microfluid Nanofluid 1 (2004): 2–21.
- Smirnova, A., Mawatari, K., Hibara, A., Proskurnin, M.A. and Kitamori, T. Micromultiphase laminar flows for the extraction and detection of carbaryl derivative. Analytica Chimica Acta 558 (2006): 69–74.
- Surmeian, M., Slyadnev, M.N., Hisamoto, H., Hibara, A., Uchiyama, K. and Kitamori, T. Three-layer flow membrane system on a microchip for investigation of molecular transport. Analytical Chemistry 74 (2002): 2014–2020.
- Tadmor, R. Line Energy and the Relation between Advancing, Receding, and Young Contact Angles Langmuir 20 (2004): 7659–7664.
- Tagawa, T., Aljbour, S., Matouq, M. and Yamada, H. Micro-channel reactor with guideline structure for organic–aqueous binary system. Chemical Engineering Science 62 (2007): 5123–5126.
- Tokeshi, M., Minagawa, T., Uchiyama, K., Hibara, A., Sato, K., Hisamoto, H. and Kitamori, T. Continuous-flow chemical processing on a microchip by

- combining microunit operations and a multiphase flow network. Analytical Chemistry 74 (2002): 1565–1571.
- Vashisth, S. and Nigam, K.D.P. Prediction of flow profiles and interfacial phenomena for two-phase flow in coiled tubes Chemical Engineering and Processing 48 (2009): 452–463.
- Versteeg, H.K. and Malalasekera, W. An introduction to computational fluid dynamics. England: Pearson Education Limited, Second edition, 2007.
- Weinmueller, C., Hotz, N., Mueller, A. and Poulikakos D. On two-phase flow patterns and transition criteria in aqueous methanol and CO₂ mixtures in adiabatic, rectangular microchannels. International Journal of Multiphase Flow 35 (2009): 760–772.
- Yamaguchi, Y., Takagi, F., Yamashita, K., Nakamura, H. and Maeda, H. 3-D Simulation and Visualization of Laminar Flow in a Microchannel with Hair-Pin Curves. AIChE Journal 50 (2004): 1530–1535.
- Yamasaki, Y., Goto, M., Kariyasaki, A., Morooka, S., Yamaguchi, Y., Miyazaki, M. and Maeda, H. Layered liquid-liquid flow in microchannels having selectively modified hydrophilic and hydrophobic walls. Korean Journal Chemical Engineering 26 (2009): 1759–1765.
- Zhao, Y., Chen, G. and Yuan, Q. Liquid-liquid two-phase flow patterns in rectangular microchannel. AIChE Journal 52/12 (2006): 4052–4060.
- Zhao, Y., Su, Y., Chen, G. and Yuan, Q. Effect of surface properties on the flow characteristics and mass transfer performance in microchannels. Chemical Engineering Science 65 (2010): 1563–1570.

APPENDICES

APPENDIX A

SIMULATION MATERIAL PROPERTIES

The properties of materials used in simulation are shown in Table A

Table A Simulation material properties

Materials	Density (kg/m ³)	Viscosity (kg/ms)
Air	1.225	1.7894e-05
Kerosene	780	0.0024
Water	998.2	0.001003
Toluene	866	0.000586

APPENDIX B

SLUG SIZE CALCULATION

The slug sizes were estimated from the simulation results in both 2D and 3D by following these six steps

1. Create the microchannel center line in the FLUENT model.
2. Plot the volume fractions against the position on the center line.
3. Calculate the interface position at volume fraction equal to 0.5 by interpolation.
4. Subtract the interface position of the water slug cap by the other side position to get the slug length.
5. Check if the slugs were uniform and average the lengths of 3 adjacent slugs.

Figure B shows the example plotted chart at water and kerosene flow rates of 10 and 20 ml/h, respectively, in 3D flow pattern and slug size validation.

Table B shows the slug length plotted in Figure 4.4. Gas and liquid phase superficial velocities (U_G and U_L) were varied to investigate the effect on the gas slug size where L_{exp} and L_{sim} are experimental and simulation results reported by Guo and Chen (2009) and $L_{sim,present}$ is present work simulation results.

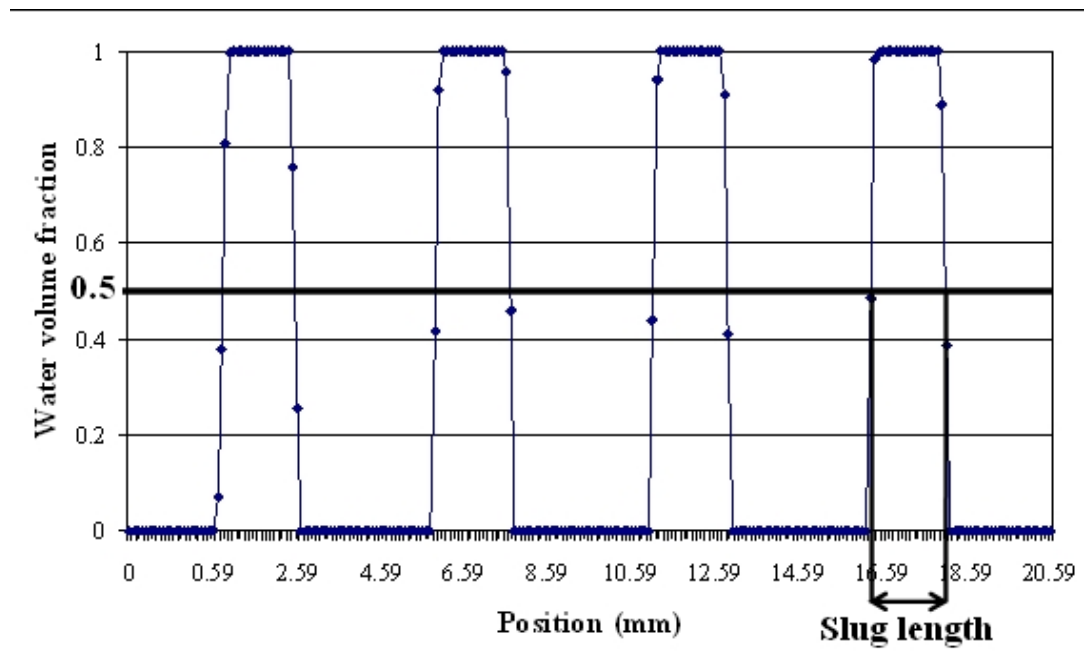


Figure B Water volume fraction at water and kerosene flow rates of 10 and 20 ml/h, respectively

Table B Simulation and reported slug length in Figure 4.4

U_G (m/s)	U_L (m/s)	L_{exp} (mm)	L_{sim} (mm)	$L_{sim,present}$ (mm)
0.0347	0.0174	1.10–1.17	1.20–1.23	1.18
0.0347	0.0694	0.47–0.49	0.51–0.54	0.55
0.0347	0.1736	0.35–0.39	0.34–0.36	0.36
0.0694	0.0764	0.73–0.76	0.70–0.72	0.70
0.0694	0.1424	0.38–0.45	0.47–0.49	0.48
0.0694	0.3472	0.21–0.22	0.22–0.23	0.27

APPENDIX C

LIST OF PUBLICATIONS

C.1 International publications

1. **Kositanont, C.**, Putivisutisak, S., Prasertdam, P., Assabumrungrat, S., Yamada, H. and Tagawa, T. Flow pattern of liquid multiphase flow in microreactors with different guideline structures. *Journal of Chemical Engineering of Japan*. 44 (2011): 649–652.
2. **Kositanont, C.**, Tagawa, T., Yamada, H., Putivisutisak, S. and Assabumrungrat, S. Effect of surface modification on parallel flow in microchannel with guideline structure. *Chemical Engineering Journal* 215-216 (2013): 404–410.

C.2 International conferences

Kositanont, C. Tagawa, T. Yamada, H. Putivisutisak, S. and Assabumrungrat, S. Effect of surface modification on parallel flow in microchannel with guideline structure. The 22nd International Symposium on Chemical Reaction Engineering, (ISCRE 22), Maastricht, The Netherlands, September 2-5, 2012 (Oral presentation).

VITA

Miss Chayanoot Kositanont was born on May 13, 1983 in Bangkok, Thailand. She received the Bachelor's Degree in Chemical Engineering from Chulalongkorn University, Bangkok, Thailand, in April 2005. After her graduation, she had done her job as a system engineer at Yokogawa (Thailand) Ltd. for 3 years. Afterward, she started her Doctoral Degree in Chemical Engineering in May 2008 under the scholarship of the Dusadeepipat fund from Chulalongkorn University. During her research years, she spent one year as an exchange student in The Nagoya University Program for Academic Exchange (NUPACE) for extending her research at Graduate School of Engineering, Nagoya University, Japan.